

Bryn Mawr College

Scholarship, Research, and Creative Work at Bryn Mawr College

Geology Faculty Research and Scholarship

Geology

2021

Vegetation effects on coastal foredune initiation: Wind tunnel experiments and field validation for three dune-building plants

Bianca Reo Charbonneau

Stephanie M. Dohner

John P. Wnek

Don Barber

Phoebe Zarnetske

See next page for additional authors

Follow this and additional works at: https://repository.brynmawr.edu/geo_pubs



Part of the Geomorphology Commons

[Let us know how access to this document benefits you.](#)

This paper is posted at Scholarship, Research, and Creative Work at Bryn Mawr College.
https://repository.brynmawr.edu/geo_pubs/23

For more information, please contact repository@brynmawr.edu.

Authors

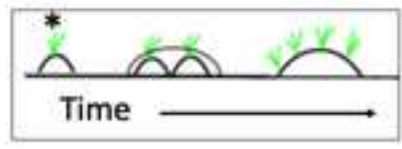
Bianca Reo Charbonneau, Stephanie M. Dohner, John P. Wnek, Don Barber, Phoebe Zarnetske, and Brenda B. Casper

Geomorphology

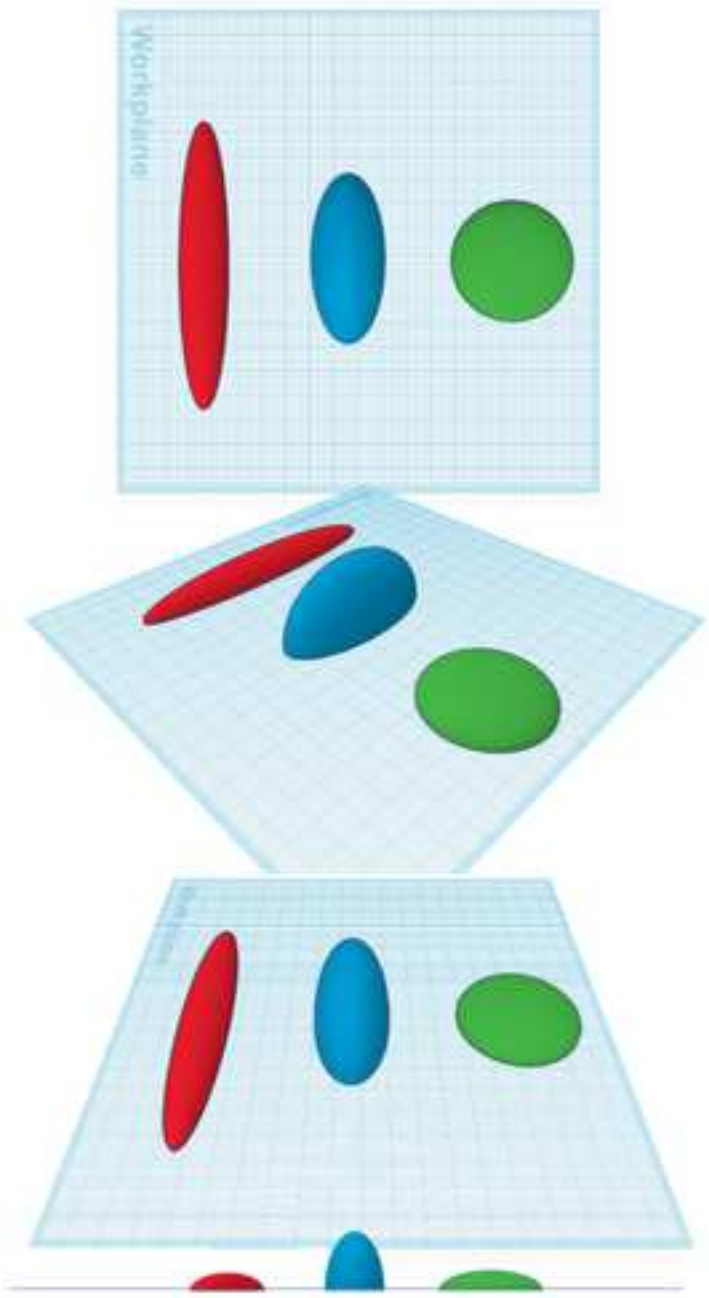
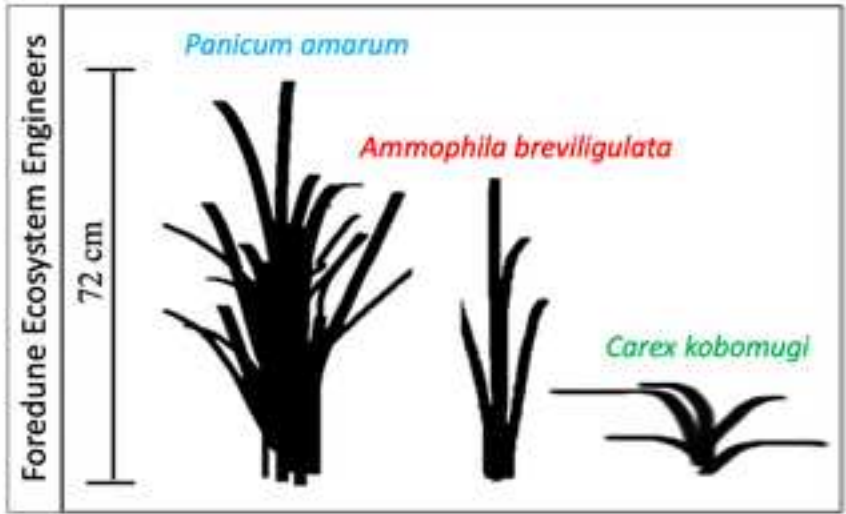
Vegetation effects on coastal foredune initiation: Wind tunnel experiments and field validation for three dune-building plants

--Manuscript Draft--

Manuscript Number:	GEOMOR-10306R2
Article Type:	Research Paper
Keywords:	Biogeomorphic and Ecogeomorphic Systems; Ecogeomorphology; Ecosystem Engineers; Nebkha
Corresponding Author:	Bianca Reo Charbonneau, BA, MS, PhD bryn mawr, PA UNITED STATES
First Author:	Bianca Reo Charbonneau, BA, MS, PhD
Order of Authors:	Bianca Reo Charbonneau, BA, MS, PhD Stephanie M. Dohner John P. Wnek Don Barber Phoebe Zarnetske Brenda Casper
Abstract:	<p>As the land-sea interface, foredunes buffer upland habitats with plants acting as ecosystem engineers shaping topography, and thereby, affecting storm response and recovery. However, many ecogeomorphic feedbacks in coastal foredune formation and recovery remain uncertain in this dynamic environment. We carried out a series of wind tunnel experiments testing how the morphology, density, and configuration of three foredune pioneer dune builder species influence the most basic stage of dune initiation — nebkha formation around individual plants. We established monocultures of native <i>Ammophila breviligulata</i> and <i>Panicum amarum</i> and invasive <i>Carex kobomugi</i> in 1m x 1m planter boxes of sand to simulate approximate natural and managed densities and planting configurations on the US Mid-Atlantic coast . We subjected each box to constant 8.25 m/s wind for 30-minutes in a moveable-bed unilateral-flow wind tunnel with an unvegetated upwind sand bed. We quantified resulting topography with sub-millimeter precision and related it to plant morphology, density, and configuration. Plant morphology, density, and configuration all influenced the resulting topography. Larger plants produced larger nebkha with greater relief, height, and sand volume. However, nebkha area, height, and planform shape varied among species, and taller plants did not necessarily produce taller nebkha. The erect grasses, <i>Ammophila</i> and <i>Panicum</i> , produced more elongated, high-relief nebkha compared to the low-lying <i>Carex</i>, which produced lower and more symmetrical nebkha. A staggered planting configuration produced greater net sediment accumulation than non-staggered. We validated these results against high-resolution field topographies of foredune nebkha and found strong agreement between the datasets. Our results provide species-specific parameters useful in designing foredune plantings and beach management and can be used to parameterize vegetation in models of foredune evolution associated with different plant species. By first understanding the underlying ecogeomorphic feedbacks involved in nebkha formation, we can more effectively scale up to forecast coastal foredune evolution and recovery.</p>



Foredune Initialization in Nebkha Formation



1 **Running head:** PLANT FOREDUNE INITIATION

2

3 **Title: Vegetation effects on coastal foredune initiation: Wind tunnel experiments and field**
4 **validation for three dune-building plants**

5

6

7 Bianca Reo Charbonneau¹, Stephanie M. Dohner², John P. Wnek³, Don Barber⁴, Phoebe

8 Zarnetske^{5,6}, and Brenda B. Casper¹

9

10 ¹Department of Biology, University of Pennsylvania, Philadelphia, PA 19104;

11 ²University of Delaware, College of Earth, Ocean, and Environment, Lewes, DE 19958;

12 ³Marine Academy of Technology and Environmental Science, Manahawkin, NJ 08050;

13 ⁴Bryn Mawr College, Departments of Environmental Studies and Geology, Bryn Mawr, PA

14 19010;

15 ⁵Department of Integrative Biology, Michigan State University, East Lansing, MI 48824

16 ⁶Ecology, Evolutionary Biology, and Behavior Program, Michigan State University, East

17 Lansing, MI 48824

18 Corresponding Author:

19 Bianca Charbonneau

20 248 Lee Circle

21 Bryn Mawr, PA, 19010

22 Email: bcharbon@sas.upenn.edu

23 Tel: (973)879-2856

24

25 **ABSTRACT**

26 As the land-sea interface, foredunes buffer upland habitats with plants acting as ecosystem
27 engineers shaping topography, and thereby, affecting storm response and recovery. However,
28 many ecogeomorphic feedbacks in coastal foredune formation and recovery remain uncertain in
29 this dynamic environment. We carried out a series of wind tunnel experiments testing how the
30 morphology, density, and configuration of three foredune pioneer dune builder species
31 influence the most basic stage of dune initiation — nebkha formation around individual plants.
32 We established monocultures of native *Ammophila breviligulata* and *Panicum amarum* and
33 invasive *Carex kobomugi* in 1m x 1m planter boxes of sand to simulate approximate natural and
34 managed densities and planting configurations on the US Mid-Atlantic coast. We subjected
35 each box to constant 8.25 m/s wind for 30-minutes in a moveable-bed unilateral-flow wind
36 tunnel with an unvegetated upwind sand bed. We quantified resulting topography with sub-
37 millimeter precision and related it to plant morphology, density, and configuration. Plant
38 morphology, density, and configuration all influenced the resulting topography. Larger plants
39 produced larger nebkha with greater relief, height, and sand volume. However, nebkha area,
40 height, and planform shape varied among species, and taller plants did not necessarily produce
41 taller nebkha. The erect grasses, *Ammophila* and *Panicum*, produced more elongated, high-relief
42 nebkha compared to the low-lying *Carex*, which produced lower and more symmetrical nebkha.
43 A staggered planting configuration produced greater net sediment accumulation than non-
44 staggered. We validated these results against high-resolution field topographies of foredune
45 nebkha and found strong agreement between the datasets. Our results provide species-specific
46 parameters useful in designing foredune plantings and beach management and can be used to
47 parameterize vegetation in models of foredune evolution associated with different plant species.
48 By first understanding the underlying ecogeomorphic feedbacks involved in nebkha formation,
49 we can more effectively scale up to forecast coastal foredune evolution and recovery.

50

51

52 **KEYWORDS:** Biogeomorphic and Ecogeomorphic Systems, Ecogeomorphology, Ecosystem
53 Engineers, Nebkha

54

55 **INTRODUCTION**

56 Ecosystem engineers directly or indirectly modify habitats by changing biotic and abiotic
57 resources or physical habitat structure (Jones et al., 1994). Plants are capable engineers,
58 physically altering environments both when living and dead (Tanner, 2001; Badano and
59 Cavieres, 2006; Bos et al., 2007; Hall et al., 2010). Vegetation is particularly important in the
60 development of coastal foredunes, defined as the shore-parallel vegetated dune ridge in the
61 backshore formed by aeolian sand deposition within vegetation (Hesp, 2002). The physical
62 geomorphological processes surrounding foredune evolution have been studied extensively

63 (Hesp and Walker, 2013; Feagin et al., 2015; Elko et al., 2016; Elko et al., 2019). Similarly, the
64 spatial variability of foredune vegetation related to geomorphological processes was appreciated
65 decades ago (Cowles, 1899; Ranwell, 1972; Carter, 1995). However, despite high investment in
66 beach-dune management efforts (Wootton et al., 2016; Elko et al., 2019), the variability and
67 mechanisms surrounding geomorphological processes and foredune vegetation have only
68 recently gained heightened research attention (e.g. Stallins, 2005; Neild and Baas, 2008;
69 Zarnetske et al., 2012; Durán Vinent and Moore, 2014; Zarnetske et al., 2015; Silva et al., 2016;
70 Goldstein et al., 2017; Feagin et al., 2019; Hacker et al., 2019; Mullins et al., 2019). Our
71 understanding of foredune ecogeomorphic feedbacks is limited (Stallins, 2006; Schlacher et al.,
72 2008; Murray et al., 2008; Corenblit et al., 2011; Stallins and Corenblit, 2018). Efforts to model
73 foredune initiation alongside storm response and recovery are thus constrained by an incomplete
74 understanding of vegetation effects (Walker et al., 2017; Jackson and Nordstrom, 2019).

75 Foredunes are non-linear, self-organizing, complex adaptive habitats categorized by
76 physical feedbacks between plants and topography (de Castro, 1995; Hesp, 2002; Neild and
77 Baas, 2008; Hesp and Walker, 2013; Balke et al., 2014; Corenblit et al., 2015). Plants create,
78 modify, and stabilize foredunes, while elevation and coastal processes (e.g. waves, overwash)
79 influence vegetation structure and succession (Stallins, 2005; Durán Vinent and Moore, 2014;
80 Zarnetske et al., 2015; Cheplick, 2016). These ecogeomorphic interactions modulate post-storm
81 foredune recovery back to a pre-storm or new system state (Bendix and Hupp, 2000; Murray et
82 al., 2008; Hesp et al., 2011; Wolner et al., 2013; Stallins and Corenblit, 2018). Aeolian sand
83 transport is steered both by topography and vegetation over a range of physical, ecological, and
84 geological timescales (Arens, 1996; Hesp et al., 2015). Across a landscape, the beach physical
85 characteristics vary (Durán Vinent and Moore, 2014; Houser and Mathew, 2011) and vegetation

86 is heterogeneously distributed (Hesp, 1989), varying in morphology and density (Arens et al.,
87 2001; Hesp et al., 2019). These characteristics create a spatiotemporally complex heterogenous
88 system (Hilton et al., 2006; Charbonneau et al., 2017; Stallins and Corenblit, 2018).

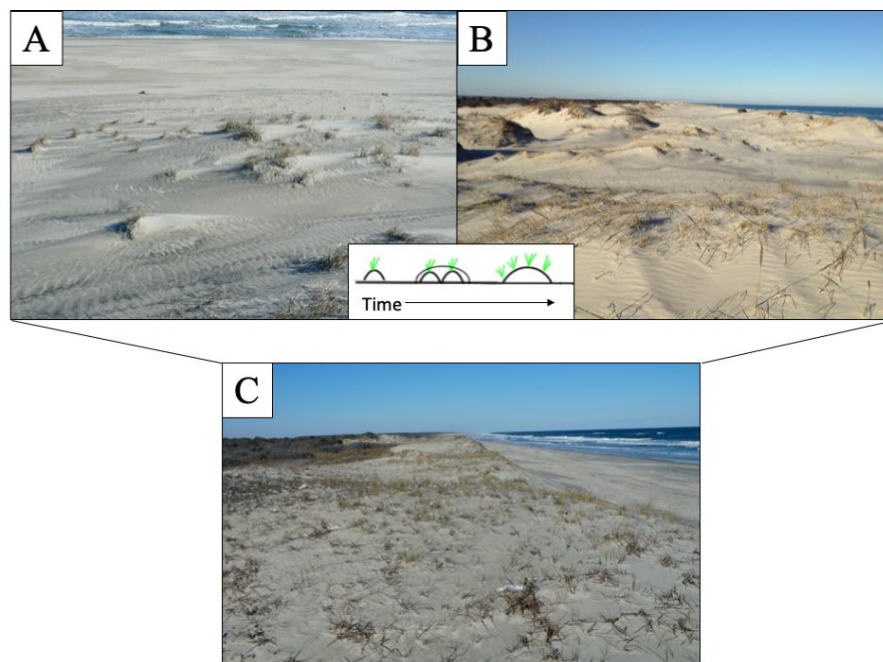
89 Topographic heterogeneity is, in part, likely due to plant species-specific morphological
90 traits impacting deposition (Hilton et al., 2006; Houser et al., 2008; Hacker et al., 2011, 2019).
91 Above- and below-ground differences in plant species morphology and growth habit can yield
92 noticeable species-level differences in the building and stabilizing of *already established*
93 foredunes (Murray et al., 2008; Hacker et al., 2011; Zarnetske et al., 2012; Duran and Moore,
94 2013, Charbonneau et al., 2016; Charbonneau et al., 2017; Hacker et al., 2019). For example,
95 some species are associated with more hummocky, erect, taller, or shorter established foredunes
96 (Davies, 1980; Hesp, 1989; Wootton et al., 2005; Hilton et al., 2006; Hacker et al., 2011;
97 Zarnetske et al., 2015; Hacker et al., 2019). Shoots create drag and surface cover, reducing wind
98 and wave erosion (Tanaka et al., 2009; Silva et al., 2016; Feagin et al., 2019) and catch sediment,
99 with species differing in capture efficiency, survival, morphology, establishment, density, and
100 root versus shoot investment (Hesp, 1989; Arens et al., 2001; Zarnetske et al., 2012; Hesp et al.,
101 2019). Changes in plant community structure can thus have cascading consequences on foredune
102 morphology and stability (Wolner et al., 2013; Charbonneau et al., 2017; Bryant et al., 2019).
103 Despite heightened coastal research since the 1960s (Jackson and Nordstrom, 2019),
104 uncertainties remain as to the underlying causes of observed topographic heterogeneity
105 associated with different plant species and densities (van Dijk et al., 1999; Arens et al., 2001; de
106 M Luna et al., 2011; Duran and Moore, 2013; Durán Vinent and Moore, 2014; Zhang et al.,
107 2015; Keijsers et al., 2016; Moore et al., 2016; Hesp et al., 2019).

108 Examining nebkha formation, one type of precursor to incipient (or embryo) foredune
109 development (Hesp, 2002; Hesp and Walker, 2013), may yield insight into what factors of plant
110 morphology and density are of greatest importance to backshore foredune initiation. Nebkha
111 form from aeolian sand deposition around discrete individuals or groups of plants, due to high
112 localized drag and reduced wind velocity (Cooke et al., 1992; Hesp, 2002; Fig. 1). Nebkha vary
113 in size from millimeters to meters, and can grow and merge over time as plants tiller and new
114 nebkha emerge (Hesp, 1989; Cooke et al., 1993; Fig. 1). This deposition can ultimately form a
115 continuous shore-parallel incipient foredune (Hesp, 1984, 1989, 2002, 2013; Fig. 1). Behind
116 plants and the nebkha body, shielding and turbulent eddies create shadow dunes or tails (Hesp,
117 1981; Hesp and Smyth, 2017). These shadow dunes can vary in size by plant and nebkha shape
118 (Raupach, 1992) and width, independent of plant height and sediment grain size (Hesp, 1981;
119 Hesp and Smyth, 2017). Shadow dune and nebkha morphology are linked, although they are
120 often examined separately (Hesp and Smyth, 2017). When nebkha are referred to in this
121 publication, the nebkha and attached shadow dune complex are grouped as one entity
122 (Charbonneau and Casper, 2018). Similar to studies of foredune ecogeomorphology, nebkha
123 research has frequently focused on established field nebkha (Gillies et al., 2014; Hesp and
124 Smyth, 2017). Nebkha can be thought of as the most basic unit or stage of foredune development
125 and as such, underlying physical-biological feedbacks that govern foredune evolution at a greater
126 scale may be illuminated from examining their initiation.

127 To examine coupled ecogeomorphic relationships of nebkha formation as foredune
128 precursors, we constructed a moveable-bed, unilateral-flow wind tunnel to test how three U.S.
129 East Coast foredune pioneer plant species and their morphological traits, planting density, and
130 planting configuration affect the initial size, shape, and volume of nebkha. We worked with

131 dominant native and invasive foredune plants at natural and managed densities and
 132 configurations. After subjecting experimental stands to wind and sediment supply conditions
 133 typical of backshore environments, we related the size and shape of each resulting nebkha to the
 134 morphological traits of their individual plants (Fig. 1A), as well as to planting density and
 135 configuration. We tested the following hypotheses: (1) Larger plants create larger nebkha; (2) a
 136 taller plant will build a taller, steeper nebkha; and (3) nebkha shape varies by plant species and
 137 not as a function of plant size, with lower-lying plants creating more circular nebkha.
 138 Furthermore, we tested the same hypotheses against quantitative field observations to evaluate
 139 the ecological relevance of our findings for sandy beaches. Our findings demonstrate that dune
 140 plant growth form, and configuration, influence nebkha size and shape. By first understanding
 141 the underlying ecogeomorphic feedbacks of nebkha formation, we can more effectively scale up
 142 to forecast foredune evolution over time and develop more effective management strategies.

143



144

145 **Fig. 1:** Foredune initiation and development over time. Field photos depict (A) small nebkha
 146 formed around individual plants on the backshore, (B) coalescence into larger nebkha containing
 147 multiple plant communities concentrated at their peaks and (C) a continuous foredune developed

148 from the merging of larger nebkha. For scale, note the size of the plants in each image which are
149 all dormant *A. breviligulata* as the images were taken in winter.

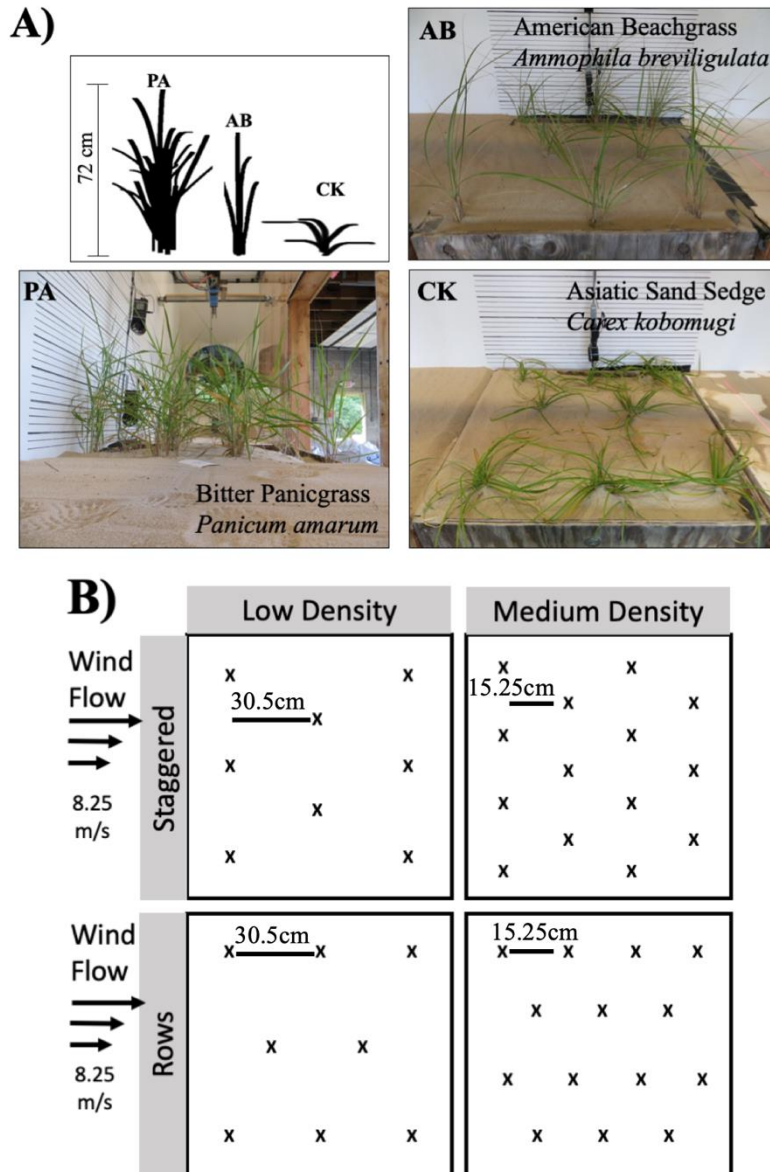
150

151 **MATERIALS and METHODS**

152 **Study Species**

153 We worked with three US East Coast dominant foredune building pioneers (Fig. 2A).

154 Erect C_3 *Ammophila breviligulata* (0.66-1 m tall), is native to the US Mid-Atlantic and Great
155 Lakes, and is a Pacific invasive grass (Hacker et al., 2011). C_4 bunchgrass *Panicum amarum* (1-2
156 m tall) is a US eastern seaboard and Gulf coast native known for high biomass production. *Carex*
157 *kobomugi* (15-30 cm tall) is an Asia native sedge, and US invasive, with a low, semi-rosette
158 growth form, small petiole angles, and blades touching or nearly touching the surface (Min,
159 2006). All are rhizomatous, spreading laterally asexually in guerilla growth form, burial-tolerant,
160 and with relatively long (15-50 cm) and narrow (<1.25 cm) leaf blades. Typical *A. breviligulata*
161 and *C. kobomugi* field densities are ≈ 40 and ≈ 140 ramets m^{-2} , respectively (Charbonneau et al.,
162 2016). *Panicum* field densities vary widely with plant age, initially having uniform density (≈ 100
163 ramets m^{-2} , 30 transects at Delaware State Seashore, September 2016), but typically thin to one
164 dense clump per m^2 (Woodhouse, 1982). *Panicum amarum* and *A. breviligulata* are available
165 commercially and planted in management efforts. *Carex kobomugi* was available and planted
166 1960-1990 in the Eastern US until its invasive qualities were documented (Wootton et al., 2005).



167
 168 **Fig. 2:** Wind tunnel experimental setup. (A) We established two native Mid-Atlantic erect
 169 grasses (AB and PA) and one invasive low-lying sedge (CK) rooted in sand in 1m x 1m
 170 monoculture plant boxes. The top left schematic is to scale, showing relative differences in plant
 171 size and morphology across species. (B) The plants were planted at low or medium density and
 172 in a staggered or non-staggered configuration relative to the prevailing wind direction. There are
 173 therefore four density x configuration treatments with four replicates in each per species.
 174

175 Wind Tunnel and Experimental Plantings

176 We constructed a moveable-bed, unilateral suction-flow wind tunnel, modified from the
 177 design of the Oregon State University O.H. Hinsdale Wave Research Lab wind tunnel (Zarnetske

178 et al., 2012). In the wind tunnel, we controlled wind velocity, wind, duration, sediment supply,
179 and grain size (Houser and Mathew, 2011), allowing us to focus on effects of varying plant
180 species, density, and configuration. The wind tunnel chamber is 6.0 m long, 1.0 m wide, and 2.0
181 m high. Near the tunnel longitudinal center, 3.6 m downwind, a 1.0 m x 1.0 m x 0.3 m wooden
182 planter box containing established and fully roots plants in sand, can be inserted and sealed flush
183 with the chamber floor. The wind tunnel is located as a research and learning tool at the Ocean
184 Country Vocation Technical School in NJ (Charbonneau and Casper, 2018). More details on the
185 wind tunnel can be found at TheWindTunnel.weebly.com. The sand used was washover sand
186 from Island Beach State Park, NJ medium quartz (mean grain size 0.300-0.350 mm). See
187 Supplementary Material S1 for grain size distributions.

188 In each planter box, we established a monoculture of rooted plants at one of three density
189 treatments and two configurations relative to wind direction. In low, medium, and high density
190 treatments, we spaced plants uniformly at 45.7 cm, 30.5 cm, and 15.25 cm apart, on center,
191 respectively (Fig. 2B). Although high density plantings reflect some field-observed densities
192 (Zarnetske et al., 2012; Charbonneau et al., 2016), this treatment produced nebkha around plant
193 groups not individuals. Therefore, these data could not be evaluated in the same manner as the
194 other densities. The high density results are included in Supplementary Material S2, but are
195 otherwise excluded from further analysis or discussion herein. The low and medium densities
196 reflect backshore Mid-Atlantic conditions and are the most common plant spacings used in dune
197 management projects (Savage and Woodhouse, 1968; Seneca et al., 1976; O'Connell, 2008;
198 Wootton et al., 2016). Within density treatments, we tested two different plant configurations.
199 Configuration 1 (2017), termed non-staggered, are planted in a regular hexagonal array oriented
200 with distinct rows parallel to flow (Fig. 2B). Configuration 2 (2018), termed staggered, is a

201 rotation of the non-staggered array 90° , producing a diagonal offset pattern (Fig. 2B). For each
202 plant species, density, and configuration, we tested four replicate boxes and four “sand-only”
203 control boxes lacking plants. See Supplementary Material S3 for images of the treatments.

204 To measure the influence of plant traits on topography, we quantified individual plant
205 morphology traits per plant before subjecting them to wind tunnel experiments. From bed-level,
206 we measured plant: (1) stem width between the two farthest stems perpendicular to the wind, (2)
207 height, bent naturally and (3) height, tallest taut leaf. We counted: (4) total leaves and (5) total
208 stems. Stem widths are not included for *C. kobomugi* as the stems tended to be buried, as they
209 often are in the field, after levelling box beds pre-experiment. Post-experiment, we cut the shoots
210 of all plants at the surface using shears and measured biomass after drying for 72 hr at 70°C .

211 To minimize wind-tunnel edge effects on saltation (Bauer et al., 2004), we only analyzed
212 nebkha buffered from the wall. All analyzed nebkha were ≥ 17 cm from the tunnel sides (Table 1)
213 and nebkha morphology data are from the central 66 cm of the tunnel (i.e., 33 cm of the
214 longitudinal centerline). Similar to many wind tunnel investigations, our experiments lacked full
215 representation of turbulent motion due to the restricted length scale (Bauer et al., 2004).
216 However, this physical limitation applied equally across all experimental treatments. Vertical
217 profiles along the chamber length and width support the formation of established and consistent
218 boundary layers. Our goal was to examine nebkha initiation in a flow setting conducive to
219 aeolian sand transport and deposition. The controlled wind tunnel environment enabled us to
220 draw robust conclusions regarding differences among treatments in conditions representative of
221 the range of fluid-sediment-vegetation interactions found in nature. Vertical and horizontal
222 velocity profiles can be seen in Charbonneau and Casper (2018) with additional higher-
223 resolution profiles throughout the wind tunnel chamber available in Supplementary Material S4.

224 **Table 1.** Number of plants versus nebkha examined per density/configuration treatment. Sample
 225 sizes are exclusive of plant and nebkha within the wind tunnel wall boundary layer. There were
 226 four replicates per species per density per configuration, staggered and non-staggered.

Box Density	Plants/Box	Non-Staggered Nebkha/Box	Staggered Nebkha/Box
Low 45.7 cm	8	2	4
Medium 30.5 cm	14	7	6

227
228

229 Wind Tunnel Experiments and Topographic Quantification

230 We conducted experiments September 2017 (non-staggered) and 2018 (staggered) with
 231 green full grown plants. We levelled a continuous dry sand bed of 2.54 cm height along the
 232 chamber and in the box using a custom rake taking care not to damage the plants. The flat
 233 upwind bed mimicked a dry sandy backshore of unlimited sediment supply for aeolian transport
 234 towards vegetation (Arens, 1996). We subjected each box to 30 min of 8.25 m/s velocity
 235 measured 60 cm above the center of the test area. We chose this speed and duration to allow
 236 maximum formation time within the bounds of our available sediment supply (≈ 25 tonnes across
 237 all boxes and runs). This speed is also consistent with the work of Zarnetske et al. (2012) and
 238 promoted accretion around the plants as opposed to scouring between plants and shielding
 239 behind plants (Järvelä, 2002).

240 Directly following the wind treatment, we quantified the topography with an industrial
 241 class II laser 3D sensor, a SICK TriSpector1060. The sensor uses triangulation and integrated
 242 data processing to collect and mesh 2500 elevation (z) profiles, every 0.42 mm, along the Y axis
 243 into a digital elevation model (DEM). Each scan encompassed 66 cm of the box width (X) the
 244 full 1 m box length (Y) plus 0.125 m upwind and downwind. It is factory calibrated, producing
 245 true XYZ mm values in all DEMs. Because Class II lasers cannot penetrate live tissue, we
 246 necessarily clipped all aboveground plant material before these scans. We extracted topographic
 247 information from the scans with SOPAS Engineering Tool V2018.3 (Intelligence, 2019).

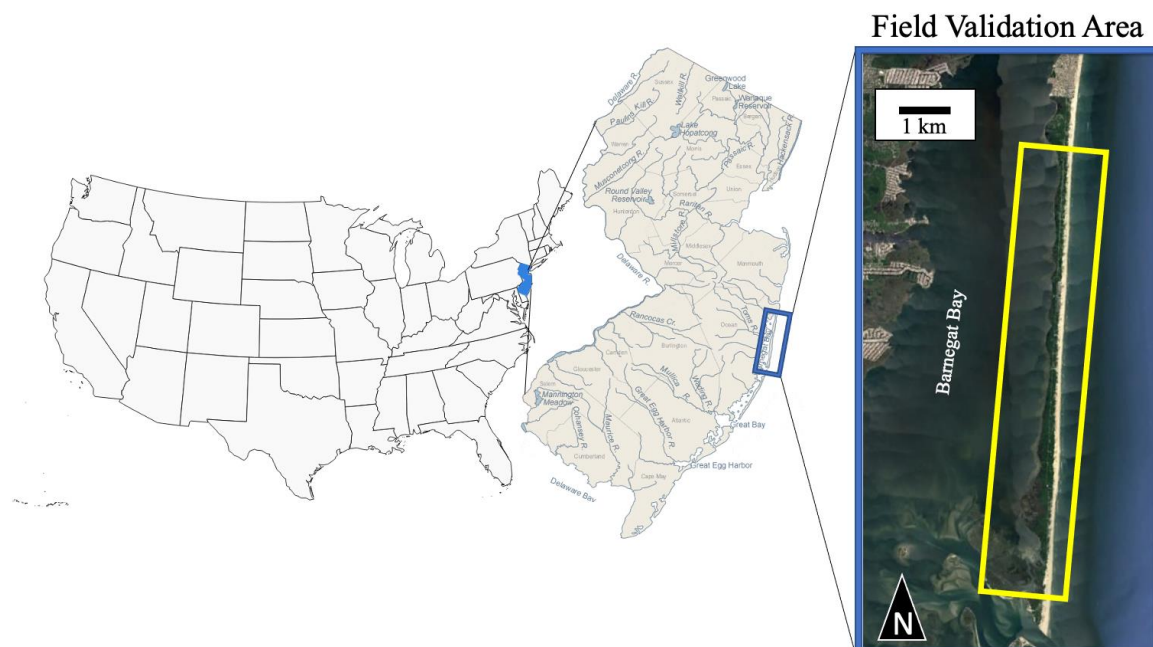
248 We also scanned each box prior to a wind tunnel run, to assess initial elevation and
249 account for any bed leveling error. We determined if erosive or accretionary forces built each
250 nebkha by examining Δz , nebkha peak height minus initial bed height. Elevation spikes in the
251 initial scans (from laser canopy reflectance) made discerning the initial upwind elevations only
252 possible in post-processing by leveling a horizontal fixed plane to the upwind sand surface in
253 SOPAS per nebkha. In 2018, we improved this quantification by also installing a vertical wire
254 stake at the front and back of each plant, marked at the sediment surface. We determined if Δz
255 reflected accretion, erosion, or was equal post-experiment with marker visibility (Supplementary
256 Material S5) and used this method to assess the accuracy of our initial scan method.

257 We quantified volume, area, elevation, and shape per nebkha in SOPAS (Intelligence,
258 2019). We defined the bounds of each nebkha from elevation point clusters where each plant was
259 located with the Blob Tool. This tool calculates basal area and volume (from object base) of each
260 blob (i.e., nebkha). Nebkha elevation is base to peak, with peak location upwind, downwind, or
261 within the plant. We measured nebkha slope from the peak and upwind extreme parallel to wind
262 flow. At the peak, we measured the width (perpendicular to flow) and length (parallel to flow) of
263 the nebkha base to quantify shape as planform eccentricity, the length/width ratio. Eccentricity
264 values closer to 1 indicate a more equant nebkha while values >1 denote a longer wind-parallel
265 axis, and <1 indicate that the wind perpendicular axis is longer than the wind parallel axis.

266 **Field Validation**

267 We quantified naturally-formed backshore nebkha at Island Beach State Park (IBSP),
268 New Jersey, USA (Fig. 3). IBSP is a ≈ 17 km micro-tidal barrier island sandy beach shoreline
269 that has never been replenished. Total annual precipitation is 127 cm. Precipitation and wind
270 speeds are lowest April-August, causing minimal sediment transport (Gares, 1992; NOAA

271 Gauge 8531680). Conversely, the Atlantic Hurricane season is June 1 to November 30, with
 272 most storms occurring September to October (Gares, 1992). The most recent notable storm to
 273 impact IBSP was Hurricane Sandy (October 2012), although other smaller storms have affected
 274 IBSP more recently (Dohner et al., 2016). Much of the foredune toe and slope have been both
 275 naturally colonized and artificially planted where nebkha and incipient dunes develop.

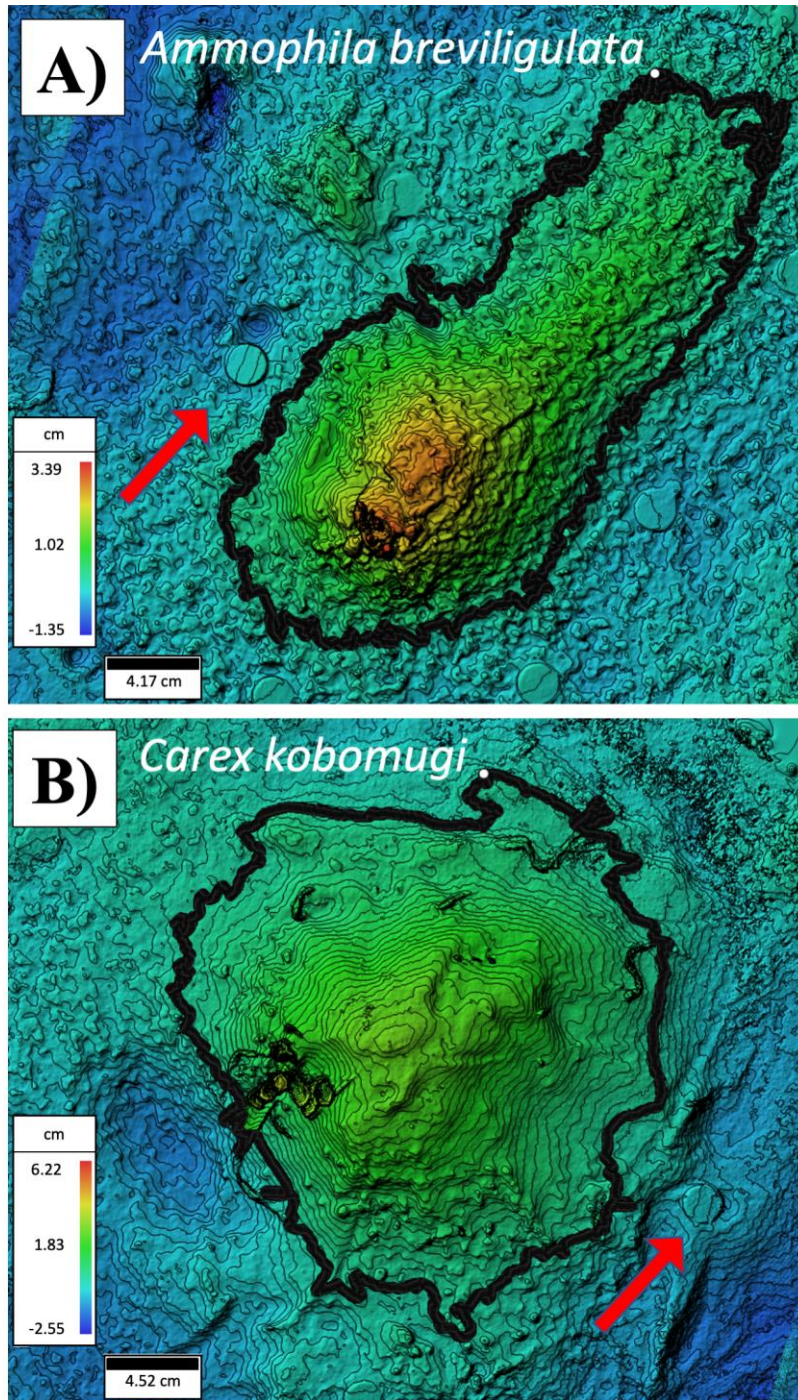


276
 277 **Fig. 3: Wind tunnel validation field site, Island Beach State Park, NJ, USA.** Field validation
 278 was carried out in the backshore along the 17 km expanse of the park (39.7975° N, 74.0976° W).
 279 Map courtesy of Google Earth.

280
 281 Fall and Spring 2018, we field truthed backshore individual *A. breviligulata* and *C.*
 282 *kobomugi* plants with the following criteria: (1) seaward of vegetation, no plants or obstructions
 283 upwind, (2) ≥ 50 cm from nearest neighbor, (3) located on flat backshore, (4) having a fully intact
 284 nebkha, and (5) being only composed of sand. We needed these criteria to establish fair
 285 comparisons between the field nebkha and our wind tunnel experiments. Specifically, we
 286 compared these data to the upwind wind tunnel plants and nebkha, which also meet these
 287 criteria. Where all conditions were met, we used pennies as ground control markers around the

288 form. The pennies, with their fixed diameter and shape, provided scale and marked locations
289 allowing for photogrammetric model accuracy checks. We measured the same plant
290 morphological traits as at the wind tunnel and then without disturbing topography, harvested the
291 aboveground biomass with garden shears. We used a 12.1-megapixel camera to collect 100
292 shadow-less photos per nebkha across all vantage points to generate one 3D model per nebkha.

293 We used Agisoft Metashape Professional Edition to create image-based 3D models of the
294 field nebkha to then quantify nebkha volume, area, and planform shape. 3D model generation
295 involved: (1) automatically aligning camera image locations; (2) manually improving camera
296 alignment with markers; (3) generating a dense point cloud; (4) defining the scale; (5) creating a
297 scale bar referenced DEM; (6) generating contours every 0.1-mm to determine nebkha and
298 backshore surface intersection; and (7) using Agisoft tools to quantify nebkha morphological
299 parameters (AgiSoft, 2018). See Supplementary Material S6 for more details and visual
300 workflow of the 3D models. We produced 3D models of 18 nebkha, five each of *C. kobomugi*
301 and *A. breviligulata*, paired spatially (< 4 m apart), and four more *A. breviligulata* (all within 5 m
302 of each other) from two locations (Fig. 4). We collected all 3D model images on the same day,
303 such that we assume all plants per location were subject to equal formative abiotic conditions.
304 We did not attempt to discern wind conditions, beyond formative direction based on nebkha
305 orientation. However, it is important to note that these nebkha would likely have developed over
306 multiple transport events with varying sediment supply (Czarnes et al., 2000; Maun, 2009; Balke
307 et al., 2014; Zarnetske et al., 2015) and multiple wetting and drying cycles occurring between
308 and among events (Czarnes et al., 2000; Maun, 2009; Balke et al., 2014; Zarnetske et al., 2015).



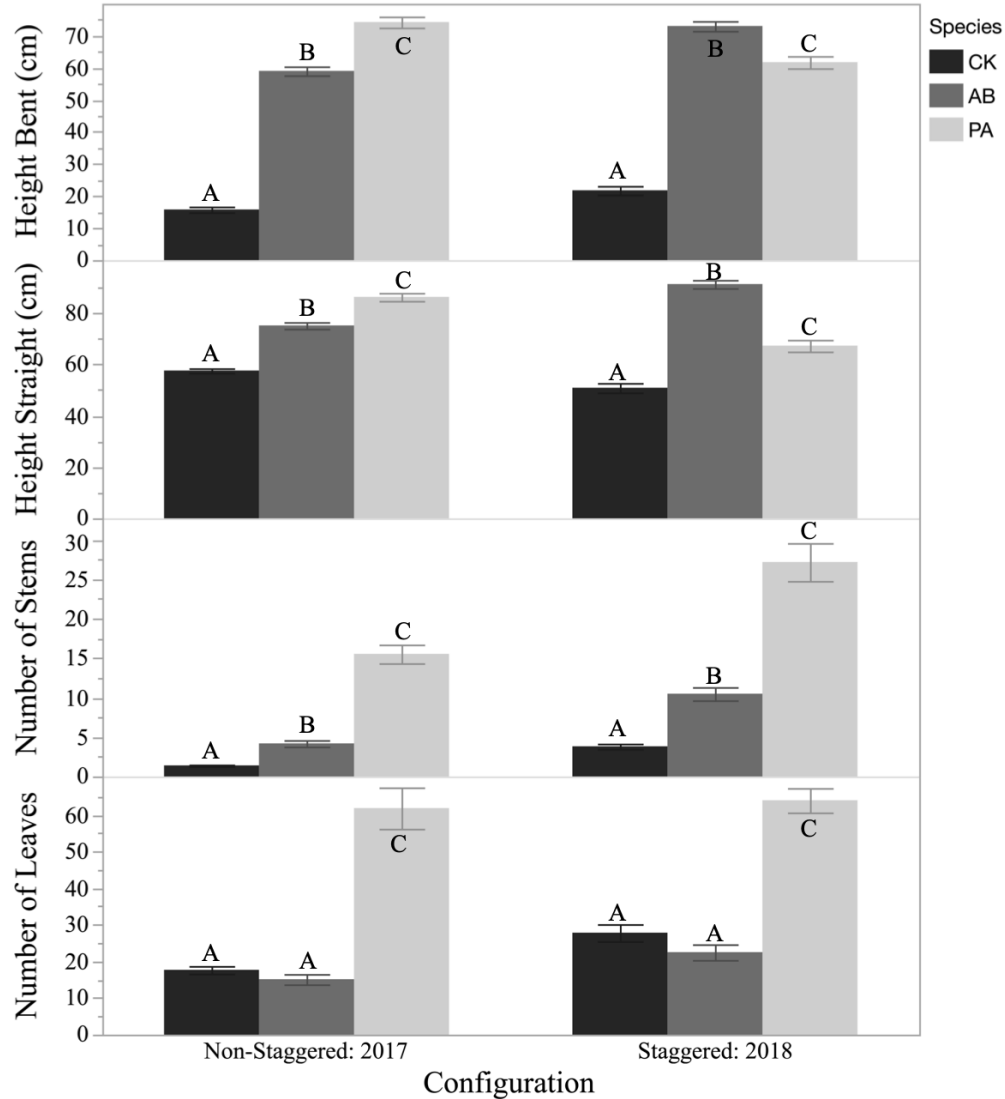
309
 310 **Fig. 4:** An example of a nebkha 3D models created from field (A) *A. breviligulata* and (B) *C.*
 311 *kobomugi*. Both in the field nebkha and wind tunnel, *A. breviligulata* produced more oblong
 312 nebkha than *C. kobomugi*, which produced more equant nebkha. The contours in both models are
 313 0.1 mm, but both models are to different vertical and horizontal scales, despite equal formative
 314 conditions, because local microtopography shaped the scale of each 3D model. The thick black
 315 line indicates the edge of the nebkha base. The red arrows each point to a penny ground control
 316 marker and represent the presumed formative wind direction based on nebkha orientation.
 317

318 **Statistical Analyses**

319 We related plant and nebkha traits, for the field truth and wind tunnel data, to test our
320 three hypotheses. We performed restricted maximum likelihood linear mixed models (LMM),
321 maintaining box (i.e., replicate) as a random effect. We performed ANCOVA of response
322 variable and treatments with species as the covariate. In any ANCOVA and linear regressions,
323 we control for a potential effect of box by examining mean results per box. All pairwise
324 comparisons are Tukey HSD. We used JMP® Pro 14 for our analyses (JMP, 2019) and
325 MATLAB® for figure 12 and our graphical abstract (MathWorks, Inc., 2018). Means are
326 reported \pm SE and all tests are two-tailed.

327 We first determined if accretionary forces built the wind tunnel nebkha. We separately
328 examined if elevation change magnitude and direction (erosion or accretion) varied by species,
329 density, plant row, and configuration with LMM. We also determined if the proportion of plants
330 producing upwind erosion versus accretion varied by species using Fisher's Exact Test.

331 We performed correlation Principal Component Analyses (PCAs) on nebkha and plant
332 variables to reduce variable dimensionality and collinearity (Graham, 2003). To determine how
333 to structure the PCAs, we first examined if plant and nebkha traits varied across treatments. We
334 performed separate LMM per plant trait examining the effect of density, species, configuration,
335 and year by species interaction. Here, configuration differences reflect varying growth conditions
336 in 2017 and 2018 (Fig. 5). We also performed nebkha trait LMMs as above. The LMMs revealed
337 consistent nebkha variation across treatments, with varying magnitudes between species. Given
338 this, we combined all treatments by constructing one PCA on plant the parameters, not including
339 stem width, and one on nebkha parameters, not including shape (Table 2).



340
 341 **Fig. 5:** Plant morphology traits across configurations reflecting differences in year. Plant traits
 342 did not vary between planting densities, but varied across species and configuration. *Carex*
 343 *kobomugi* (CK) was consistently the smallest plant in all metrics. Note that in 2017 *P. amarum*
 344 (PA) was taller than *A. breviligulata* (AB), but in 2018 this relationship flipped. Error bars
 345 represent \pm SE with different letters above species representing statistically different means from
 346 Tukey HSD pairwise comparisons.

347
 348 We largely tested our hypotheses based on the PC partial contributions of variables and
 349 loading magnitude and direction (Table 2). All variables loading on both plant and nebkha PC1
 350 contributed in a similar positive way to the respective PC1 score, equating to greater PC1 scores
 351 indicates a larger nebkha and plant with respect to all variables (Table 2). Nebkha PC2 represents
 352 nebkha relief, or height relative to area inversely related, greater values represent taller nebkha

353 with a smaller area (Table 2). We examined if nebkha PC1 and PC2 varied between species with
 354 LMM. To test Hypothesis (1), that nebkha size varies by plant size (plant PC1), we performed
 355 two ANCOVA analyses, with nebkha PC1 and volume (normalized via log transformation) as
 356 the independent variables; we further examined species differences with a Wilcoxon Rank Sum
 357 Test. For Hypothesis (2), that a taller plant builds a taller nebkha, we tested if nebkha PC2
 358 variation was explained by plant size (plant PC1). Similarly, we examined nebkha height and
 359 PC2 in the grasses in an LMM as a function of species, year, and their interaction knowing *P.*
 360 *amarum* was tallest 2017, but *A. breviligulata* was tallest 2018. To test Hypothesis (3), nebkha
 361 planform shape varies by plant species, we performed two LMM, one to test variation by density,
 362 configuration, and species and another by size (plant PC1) and species. We compared nebkha
 363 shape across species with Kruskal-Wallis, and Steel-Dwass pairwise comparisons.

364
 365 **Table 2.** Loadings and relative contribution of the morphology variables for both the nebkha and
 366 plant PCA. We performed a PCA separately on plant and nebkha morphology traits The
 367 eigenvalues are λ and the values in parentheses represent the percentage of variability explained
 368 by each variable in the PC and in its axis (λ). The PCA accounted for 96.9% and 90.8% of the
 369 variability in nebkha and plant morphology, respectively.

	Variable	Principal Component 1		Principal Component 2	
		Loading Score	λ	Loading Score	λ
Nebkha	Height	0.81 (27.4%)	2.37 (79.0%)	0.58 (63.8%)	0.54 17.9%
	Volume	0.97 (39.5%)		-0.09 (1.62%)	
	Area	0.89 (33.1%)		-0.43 (34.6%)	
Plants	# Leaves	0.74 (22.3%)	2.46 (61.5%)	0.58 (28.3%)	1.17 29.3%
	# Stems	0.80 (25.9%)		0.50 (21.4%)	
	Height (Taut)	0.72 (21.1%)		-0.65 (35.7%)	
	Height (Natural)	0.87 (30.7%)		-0.41 (14.7%)	

370 We used Wilcoxon Signed-Rank tests to compare plant traits, and likewise, nebkha traits,
371 between wind tunnel and field data. As previously mentioned, to ensure fair comparison between
372 field and wind tunnel nebkha, we only compared field nebkha ($n = 13$) to wind tunnel nebkha
373 that were in the first upwind row in both densities for *A. breviligulata* ($n = 21$). Specifically, for
374 *C. kobomugi*, we only used upwind low density wind tunnel data to also maintain a more
375 balanced sample size between field ($n = 5$) and wind tunnel replicates ($n = 7$). We separately
376 compared nebkha height, area, volume, and planform shape between field and wind tunnel (1) *A.*
377 *breviligulata* nebkha, (2) *C. kobomugi* nebkha, and (3) then explicitly compared *A. breviligulata*
378 and *C. kobomugi* field nebkha pairs. As stated above, we used PCA and regression to test our
379 three hypotheses, but only for *A. breviligulata* given the $n = 5$ field sample size for *C. kobomugi*.

380

381 RESULTS

382 Plant Morphological Differences Across Treatments

383 The LMMs revealed that no plant traits differed between planting densities, but
384 highlighted species differences in morphology and size 2017 and 2018. Generally, for most
385 metrics *Carex* was smallest and *Panicum* was largest (Fig. 3). Both years, *Ammophila* had an
386 equal number of leaves as *Carex*, and *Panicum* had more stems than both ($F_{2,44} = 48.9$, $P <$
387 0.0001). Both years, *Carex* had the least number of stems and *Panicum* had the most ($F_{2,32} =$
388 80.02 , $P < 0.0001$) with all species having more stems in 2018 than 2017 ($F_{1,44} = 15.3$, $P <$
389 0.001). The two height metrics were equal across years, but there was a species X year
390 interaction indicating that *Carex* was shortest both years, but in 2017 *Ammophila* was taller than
391 *Panicum* ($F_{2,45} = 44.61$, $P < 0.0001$) whereas in 2018 *Panicum* was taller than *Ammophila* ($F_{2,42}$

392 = 205.51, $P < 0.0001$). Stem widths in *Panicum* and *Ammophila* were statistically equal across
 393 years with *Panicum* stems wider than *Ammophila* stems ($F_{1,28} = 22.7$, $P < 0.0001$).

394

395 *Wind Tunnel Nebkha Formation*

396 Nebkha only formed in treatments containing plants. In the control boxes without plants,
 397 transverse aeolian ripples of uniform size and shape formed. Elevation change per nebkha varied
 398 by species ($F_{2,45} = 5.83$, $P = 0.005$), and was greater for *P. amarum* (7.21 ± 1.04 mm) than for *A.*
 399 *breviligulata* (2.38 ± 1.0 mm). Change in elevation was also influenced by density ($F_{1,45} = 6.70$,
 400 $P = 0.01$) and configuration ($F_{1,45} = 9.59$, $P < 0.005$). Regardless of species, nebkha in the non-
 401 staggered medium density treatment had less elevation change than other treatments. Plants with
 402 upwind erosion had less elevation gain (5.11 ± 0.58 mm) than those accreting upwind ($7.43 \pm$
 403 0.90 mm; $F_{1,15} = 5.59$, $P = 0.02$). *Carex kobomugi* nebkha were formed by both upwind and
 404 downwind deposition whereas the two erect grasses predominantly had upwind scouring and
 405 downwind accretion (species comparison $DF = 2$, $\chi^2 = 23.76$, $P < 0.001$; Supplementary Material
 406 S5). Regardless of configuration or density, the peaks of *A. breviligulata* (87 %) and *P. amarum*
 407 (66 %) nebkha were largely leeward versus split between upwind and downwind for *C.*
 408 *kobomugi* (51 %; Supplementary Material S5). Nebkha ranged in upwind and downwind slope 1-
 409 16° ($\bar{x} = 7.65 \pm 0.22^\circ$), not reaching the assumed angle of repose $\sim 30^\circ$.

410

411 *Wind Tunnel Nebkha Differences Across Treatments*

412 Planting density did not statistically impact nebkha traits, but configuration did.
 413 Staggered treatments consistently produced larger nebkha in all size parameters, area ($F_{1,32} =$
 414 23.67 , $P < 0.0001$), height ($F_{1,37} = 8.02$, $P < 0.01$), and volume ($F_{1,38} = 18.61$, $P < 0.0001$).

415 Nebkha planform shape did not vary between density or configuration treatments. The staggered
 416 configuration produced nebkhah of approximately double the volume of the non-staggered
 417 configuration across all species (Table 3). For *C. kobomugi* and *A. breviligulata*, the staggered
 418 configuration produced nebkhah with ~2x larger area than the non-staggered configuration.
 419 Planting row (i.e., front, back, middle) did not affect nebkhah PC1 or PC2. Basal/frontal area
 420 varied between species and densities, but was not quantified (Supplementary S3).

421 **Table 3.** Staggered planting configuration produced larger nebkhah across all size metrics with
 422 variations in magnitude across species. Results are LMM holding box as a random effect and
 423 means are reported \pm S.E.

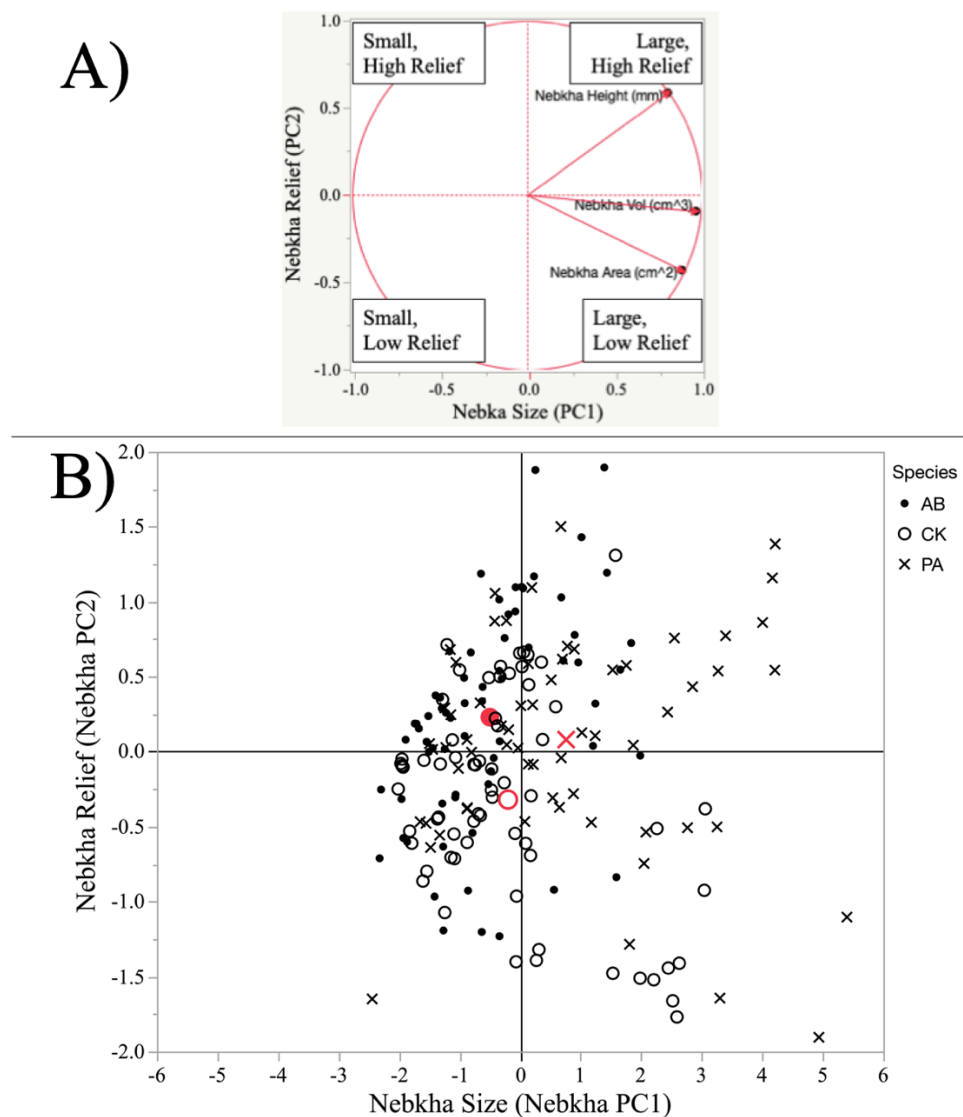
	Species	Staggered	Non-Staggered	Species Effect	Configuration Effect
Nebkha Volume	<i>A. breviligulata</i>	19.15 \pm 2.16 cm ³	10.77 \pm 2.41 cm ³	<u>(CK = AB) < PA</u> F _{1,38} = 13.75, P < 0.0001	F _{1,38} = 18.61, P < 0.0001
	<i>P. amarum</i>	41.15 \pm 3.88 cm ³	22.79 \pm 4.44 cm ³		
	<i>C. kobomugi</i>	22.83 \pm 3.19 cm ³	13.32 \pm 3.43 cm ³		
Nebkha Height	<i>A. breviligulata</i>	7.26 \pm 0.44 mm	6.50 \pm 0.44 mm	<u>(CK = AB) < PA</u> F _{1,37} = 8.61, P < 0.001	F _{1,37} = 8.02, P < 0.01
	<i>P. amarum</i>	9.45 \pm 0.50 mm	7.01 \pm 0.49 mm		
	<i>C. kobomugi</i>	6.45 \pm 0.32 mm	5.88 \pm 0.38 mm		
Nebkha Area	<i>A. breviligulata</i>	55.28 \pm 4.67 cm ²	42.31 \pm 5.75 cm ²	<u>(PA = CK) > AB</u> F _{1,32} = 9.35, P < 0.001	F _{1,32} = 23.67, P < 0.0001
	<i>P. amarum</i>	108.97 \pm 10.05 cm ²	65.23 \pm 11.31 cm ²		
	<i>C. kobomugi</i>	95.02 \pm 10.32 cm ²	52.31 \pm 6.05 cm ²		

424

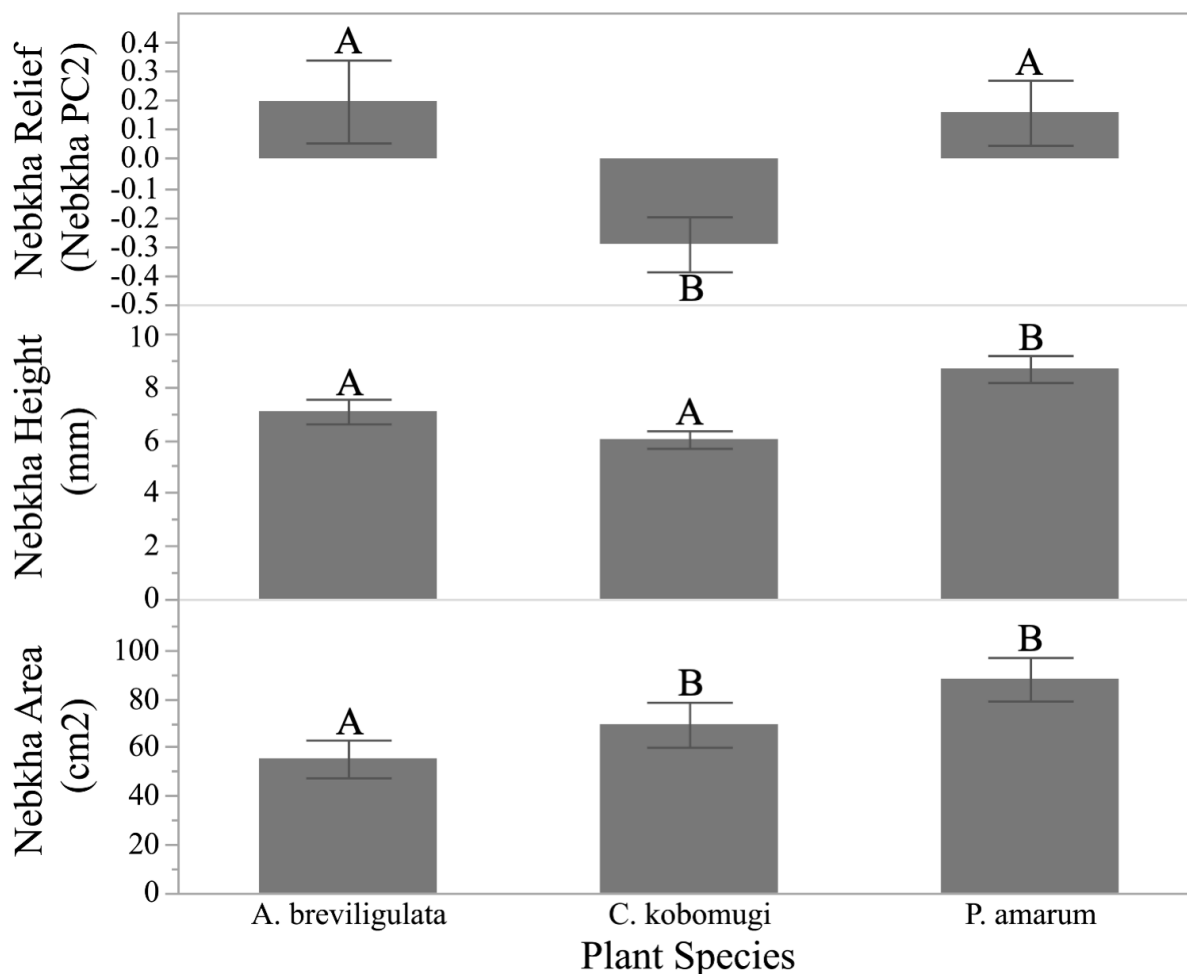
425 Wind Tunnel Nebkha Differences Across Species

426 Ordination plots of nebkhah PCAs highlight species differences in nebkhah size and relief
 427 (Fig. 6). Examining nebkhah PC1, both *Ammophila breviligulata* and *C. kobomugi*, produced
 428 smaller nebkhah than *P. amarum* (F_{2,41} = 8.21, P = 0.001). Examining nebkhah height relative to
 429 surface area (nebkhah PC2), *C. kobomugi* produced nebkhah of lower relief and greater surface
 430 area, than both erect grasses which produced nebkhah of statistically equivalent relief (F_{2,38} =
 431 7.38, P < 0.01). LMM revealed that this result is driven by *C. kobomugi* and *P. amarum*
 432 producing nebkhah of equivalent area (F_{1,32} = 9.35, P < 0.001), but *C. kobomugi* and *A.*

433 *breviligulata* nebkha being equivalent in height ($F_{1,37} = 8.61$, $P < 0.001$; Fig. 7). Amount of
 434 biomass upwind of a plant did not impact nebkha PC1 (ANCOVA $P > 0.05$).



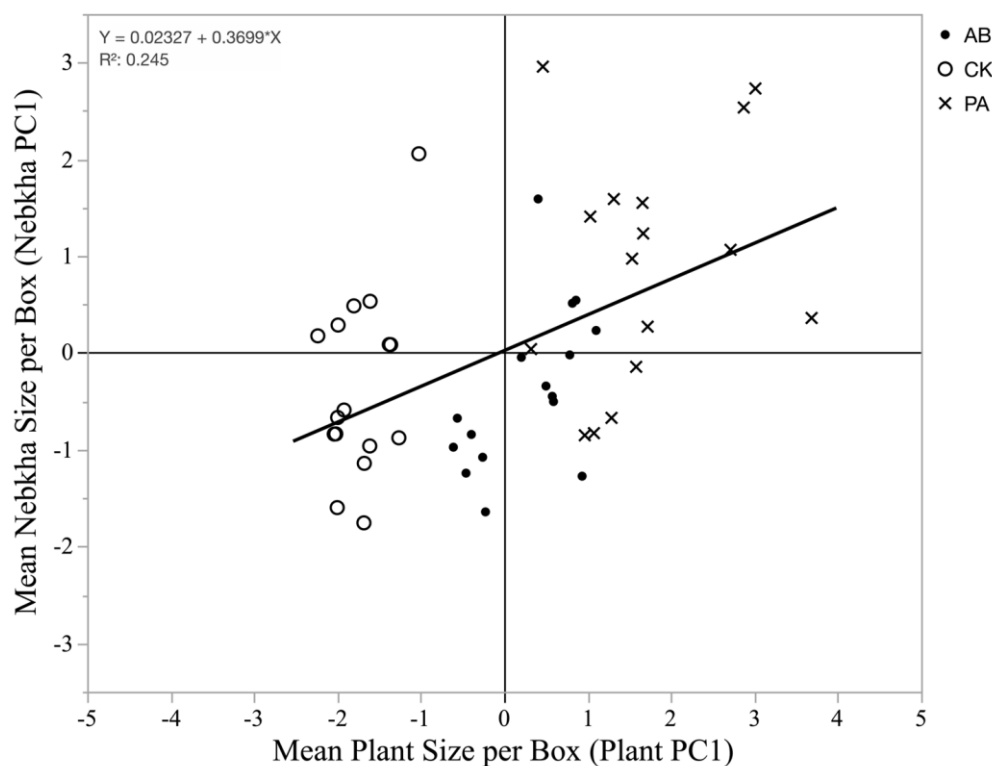
435
 436 **Fig. 6:** Variation in nebkha size and shape across plant species explained by PCA. (A)
 437 Contribution of variables to the two principal components describing the variability in nebkha
 438 traits: volume, area, and height. PC1, loads fairly equally across all variables such that nebkha
 439 with large PC1 are of a larger size. PC2 loads heavily on nebkha height (negatively) and surface
 440 area (positively) as inverses, representing relative relief such that larger PC2 indicates greater
 441 relief than smaller PC2. (B) The ordination plot highlights species-specific differences in the size
 442 and relief of nebkha across species. Red points represent the mean for each species.
 443



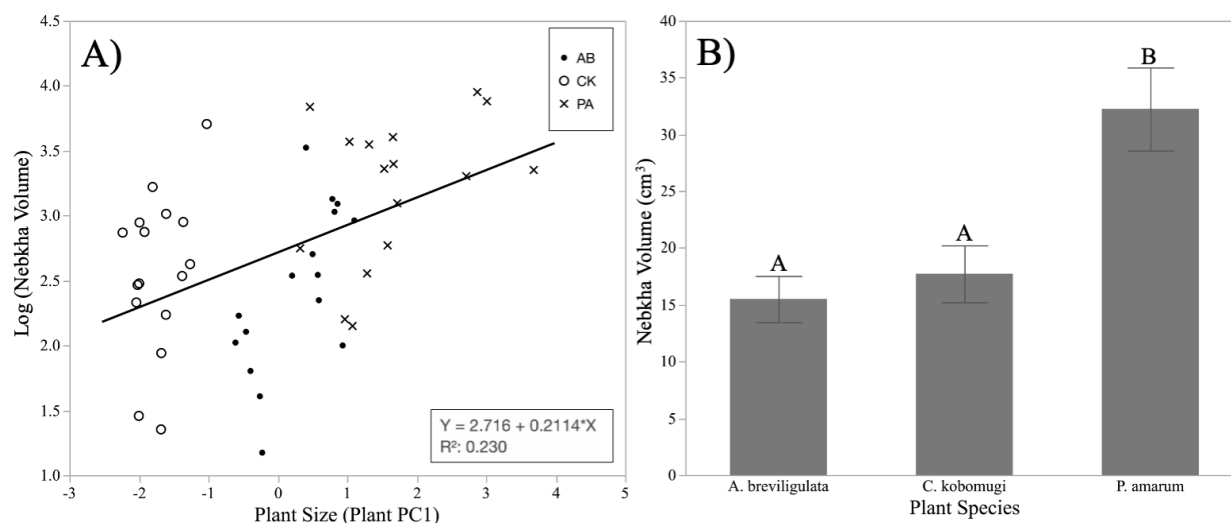
444 **Fig. 7:** Nebkha relief across plant species. Relief varied as a function of nebkh height and area
 445 across species with *C. kobomugi* creating nebkh representative of both erect grasses. Nebkha
 446 PC2 represents, as inverses, nebkh area (+) relative to height (-). *Carex kobomugi* nebkh had
 447 lower PC2 than both erect grasses, but examining the two variables loading on it, *C. kobomugi*
 448 produced equal nebkh height as the smaller erect grass *A. breviligulata* and equal area to the
 449 larger erect grass *P. amarum*. Error bars represent \pm SE with different letters above species
 450 representing statistically different means from Tukey HSD pairwise comparisons. Means shown
 451 are mean value per box.
 452
 453

454 ANCOVA revealed that nebkh size (nebkh PC1) increased linearly with plant size
 455 (plant PC1), demonstrating that larger plants produced larger nebkh ($F_{1,44} = 5.47$, $P = 0.02$; Fig.
 456 8). The slope and direction of this relationship did not significantly differ between species
 457 indicating a universal positive relationship between plant size and nebkh size between the
 458 species (Fig. 8). Similarly, larger plants, (i.e., greater plant PC1) built nebkh of greater log

459 volume ($F_{3,44} = 9.48$, $P < 0.0001$). The slope of this relationship did not vary between the species
 460 although mean log nebkha volume did vary by species ($F_{2,44} = 5.89$, $P < 0.01$). *Carex kobomugi*
 461 and *A. breviligulata* produced nebkha of equivalent volume ($F_{1,38} = 13.75$, $P < 0.0001$), both
 462 smaller than *P. amarum* (Wilcoxon Rank Sum; $\chi^2 = 12.69$, $DF = 2$, $P < 0.01$; Fig. 9).



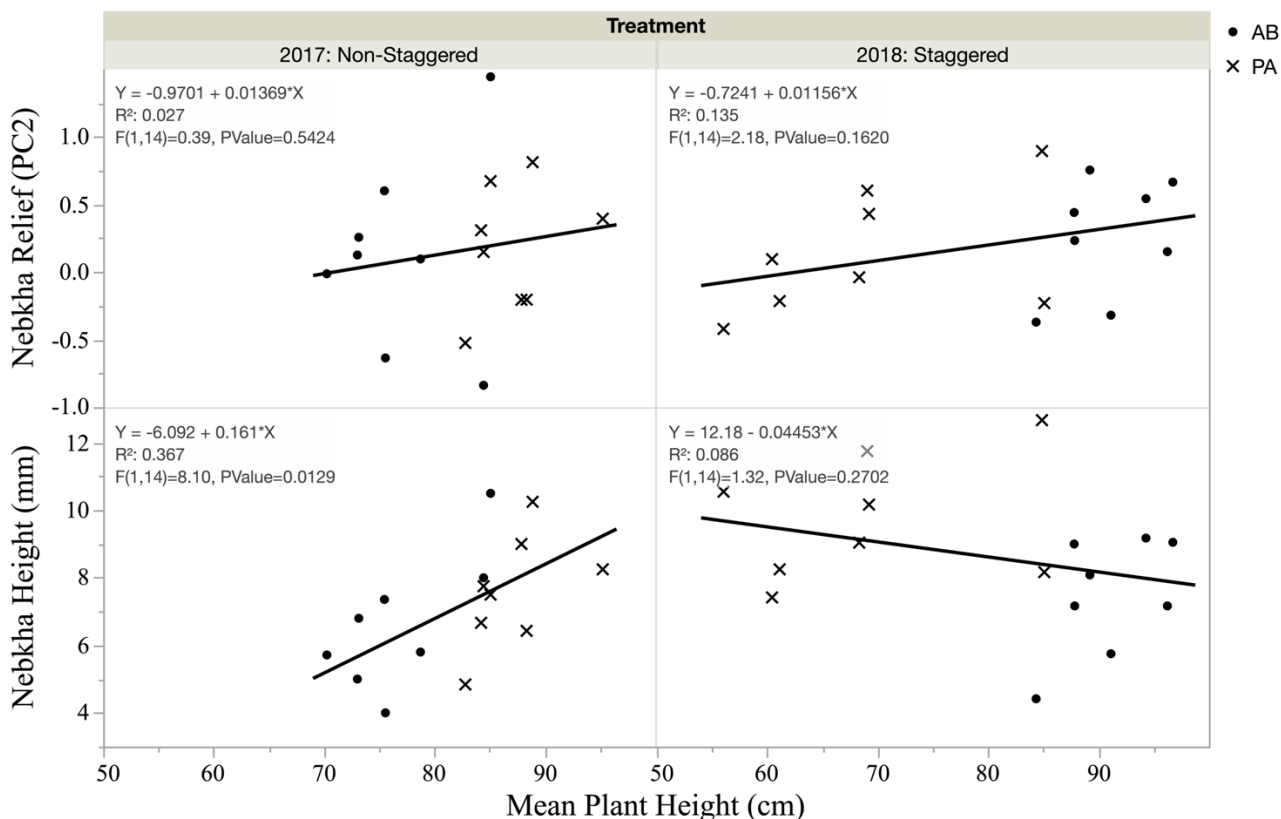
463
 464 **Fig. 8:** Ordination plot of plant PC1 and nebkha PC1. Larger values for both axes indicate larger
 465 plants and nebkha, respectively, such that there is a positive linear relationship between plant
 466 size and nebkha size.
 467



468
 469 **Fig. 9:** Nebkha volume and plant species and identity. Nebkha volume increased with increasing
 470 plant size with the largest plant species, *P. amarum* (PA) producing the largest nebka. (A) All
 471 plants had increasing log (nebka volume) with the same slope across species with (B) the
 472 largest plant, *P. amarum* (PA) producing nebka of greater volume than *A. breviligulata* (AB)
 473 and *C. kobomugi* (CK). (A) The data are normalized with log transformation and mean volume
 474 per box is used to control for box as a potential confounding factor.

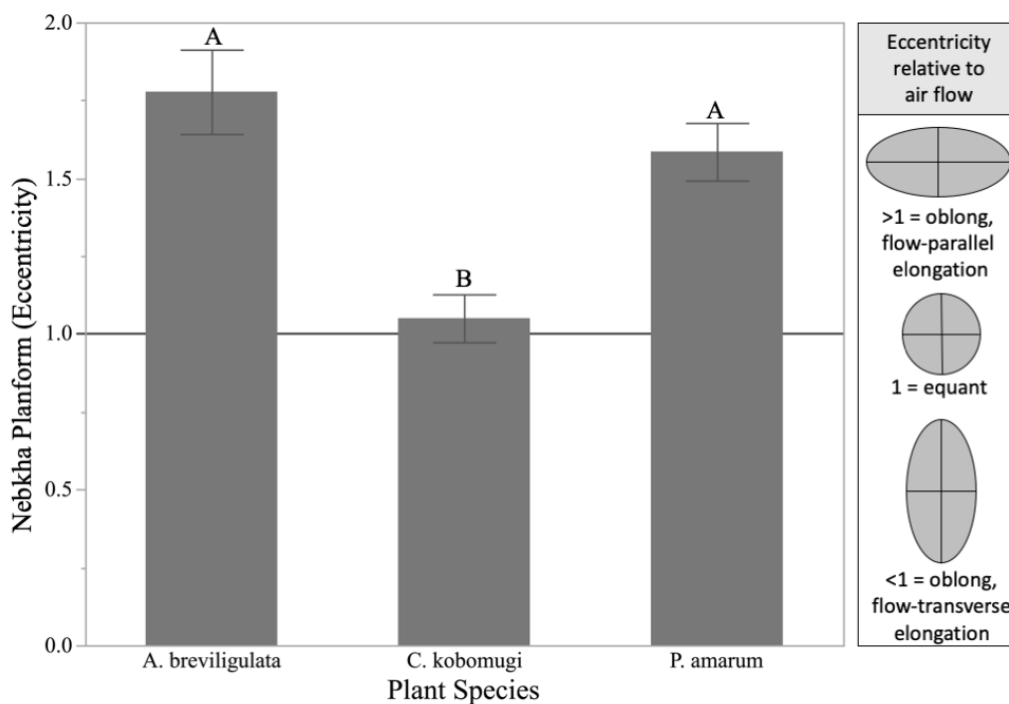
475
 476 No clear pattern emerged supporting taller plants building taller nebka. Nebkha PC2,
 477 representing nebka area relative to height (Table 2), was unrelated to plant size (PC1), but
 478 varied by species. Recall that in 2017, *P. amarum* was taller than *A. breviligulata*, but in 2018 *P.*
 479 *amarum* < *A. breviligulata* (Fig. 5). However, among these species there is no year by type
 480 interaction with nebka height ($F_{1,25} = 1.56$, $P = 0.22$) or nebka PC2 ($F_{1,25} = 0.01$, $P = 0.89$; Fig.
 481 10). Nebkha PC2, height relative to surface area, did not vary between the two erect grasses ($P =$
 482 0.53), and nebka created by *P. amarum* were taller both years despite which species was taller
 483 ($F_{1,25} = 5.78$, $P = 0.02$; Fig. 10). Nebkha height is better explained by plant width than height as
 484 LMMs revealed that a wider stem base produced taller nebka both in the field for *A.*
 485 *breviligulata* ($F_{1,1} = 5.44$, $P = 0.04$) and in both erect grasses in the wind tunnel regardless of
 486 species (LMM: $F_{1,129} = 7.98$, $P < 0.01$). Maximum nebka height achieved was 16 mm.

487

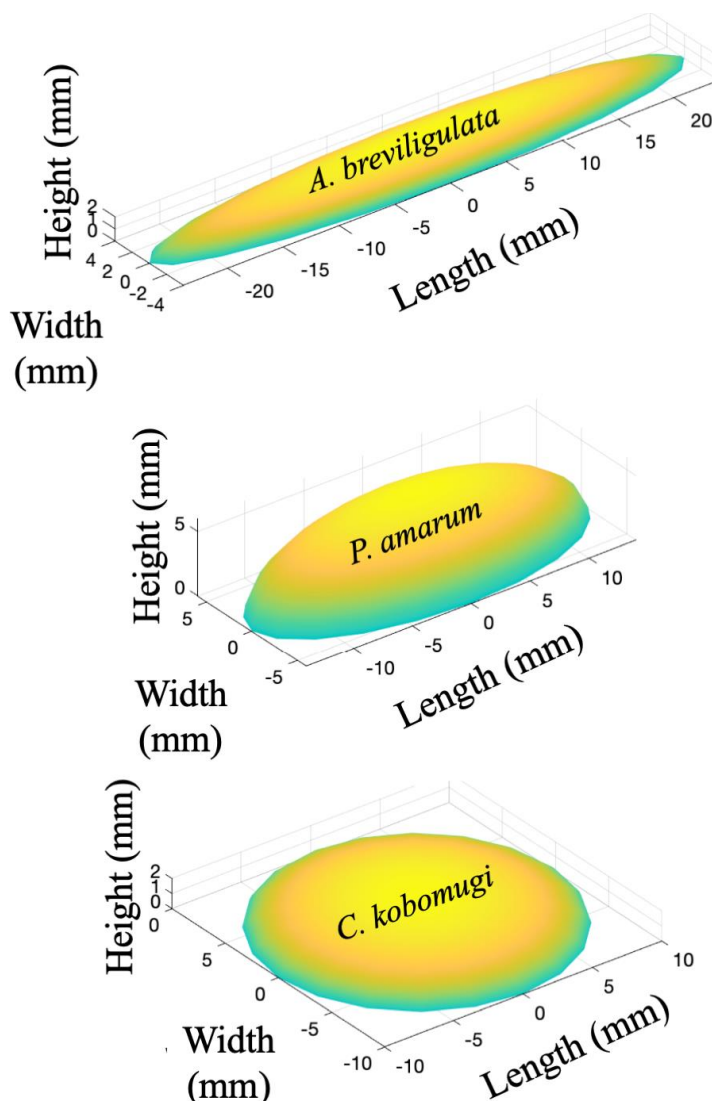


488
 489 **Fig. 10: Nebkha height relative to plant height.** A taller plant does not necessarily build a
 490 taller nebka as seen in the erect grasses *P. amarum* (PA) and *A. breviligulata* (AB). Nebkha
 491 height and relative relief (PC2: nebka area (+) relative to height (-) as inverses) were both
 492 unrelated to plant height except for in 2017 when PA was taller than AB. However, we do not
 493 see the same relationship in 2018 when AB was taller than PA suggesting that this relationship is
 494 due to other factors of plant morphology. The values represent the mean per box replicate to
 495 control for box as a potential confounding factor.
 496

497 Nebkha planform shape did not vary by treatment, density ($P = 0.54$), configuration ($P =$
 498 0.42) or plant size ($P = 0.85$), but varied by species ($F_{2,32} = 12.55$, $P < 0.0001$). *Carex kobomugi*
 499 created equant, fairly circular nebka. The two erect grasses, which did not differ in nebka
 500 shape, produced oblong planar nebka, with flow-parallel elongation relative to wind direction
 501 (Fig. 11 and 4; Table 3). Mean representations of the nebka produced by the three plant species
 502 are shown in Fig. 12. Examining LMM, no one morphological trait explained nebka shape.



503
 504 **Fig. 11:** Wind tunnel nebkha shape across plant species. Eccentricity is the ratio of the length
 505 and width of nebkha such that values > 1 are longer than wider and values of 1 are equally long
 506 and wide along the prevailing wind direction. *Carex kobomugi* consistently produced more
 507 equant nebkha whereas the erect grasses, *P. amarum* and *A. breviligulata*, produced oblong or
 508 more planar nebkha. Different letters above species represent statistically different means from
 509 Tukey HSD pairwise comparisons.
 510



511 **Fig. 12:** To scale idealized representation of wind tunnel nebkha created by the three different
 512 foredune plant species. Nebkha differences were consistent across planting densities. The
 513 dimensions shown are based on the overall means for each plant species across density and
 514 configuration treatments. It is important to note that although these nebkha are small, our field
 515 validation data suggest these shape and size differences accrue as the nebkha grow larger.
 516

517
 518 *Field Validation: Field Nebkha Examinations*

519 Field *A. breviligulata* nebkha were larger than those produced in the wind tunnel, but
 520 they were equal in planform shape and held the same observed relationships between plant and
 521 nebkha morphology as in the lab setting. Field nebkha displayed greater area, height, and volume
 522 (Table 4), despite wind tunnel *A. breviligulata* having more biomass. All *A. breviligulata* nebkha
 523 were oblong (longer tails relative to width) but the length to width ratio was greater in the field

524 nebkha (Table 4). Plant and nebkha PC1 were positively linearly related in that larger plants
 525 created larger nebkha ($F_{1,11} = 6.31$, $R^2 = 0.36$, $P < 0.03$). Similarly, nebkha volume increased
 526 with greater plant size (PC1; $F_{1,11} = 5.11$, $R^2 = 0.32$, $P < 0.05$). Plant height was unrelated to
 527 nebkha height while plant size (PC1) was unrelated to nebkha relief (i.e., height versus area).

528 **Table 4.** The *A. breviligulata* plants that formed the field nebkha were smaller than those in the
 529 wind tunnel, but they produced larger nebkha than in the wind tunnel. Nebkha shape was
 530 elongated in the wind tunnel and field, but field nebkha had greater elongation relative to their
 531 width parallel to the prevailing wind. N = 13 for each dataset.

	Field <i>A. breviligulata</i> Nebkha	Wind Tunnel <i>A. breviligulata</i> Nebkha	Wilcoxon Rank Sum Test
Dry Biomass	1.68 ± 0.37 g	6.26 ± 0.90 g	Z = -3.98, P < 0.0001
Nebkha Area	331.90 ± 78.69 cm ²	56.26 ± 6.66 cm ²	Z = 4.52, P < 0.0001
Nebkha Height	18.4 ± 1.58 mm	7.16 ± 0.62 mm	Z = 4.56, P < 0.0001
Nebkha Volume	69.2 ± 23.5 cm ³	16.4 ± 2.5 cm ³	Z = 2.92, P < 0.001
Nebkha Shape	3.01 ± 0.40	1.87 ± 0.34	Z = 3.36, P < 0.001

532
 533 Field *C. kobomugi* nebkha were larger than wind tunnel nebkha although planform shape
 534 was equal. Specifically, field nebkha had greater area (Z = 2.76, P < 0.01), volume (Z = 2.27, P
 535 = 0.02), and trended towards being taller (Z = 1.85, P = 0.06), despite *C. kobomugi* plants in the
 536 wind tunnel having greater biomass (Z = 1.79, P = 0.05). Although field nebkha were larger than
 537 those in the wind tunnel, nebkha planform shape was equivalent ($\bar{x} = 1.18 \pm 0.25$, P = 0.10).

538 Consistent with wind tunnel findings, field nebkha did not vary between paired
 539 individuals of *A. breviligulata* and *C. kobomugi* in area, height, or volume, but varied in
 540 planform shape. Field *A. breviligulata* produced elongated ellipses with longer tails parallel to
 541 the wind compared to *C. kobomugi*, which produced more uniform, round nebkha ($\bar{x}_{AB} = 2.46 \pm$
 542 0.17 , $\bar{x}_{CK} = 1.44 \pm 0.16$, Z = -2.51, P = 0.01; Fig. 4). These results are consistent with findings in
 543 the wind tunnel, where nebkha formed by *A. breviligulata* and *C. kobomugi*, with no plants

544 upwind of them, did not vary in nebkha area, height, angle or volume, but did vary in shape (\bar{x}_{AB}
545 = 1.93 ± 0.35 , $\bar{x}_{CK} = 1.25 \pm 0.19$, $Z = -2.14$, $P = 0.03$).

546

547 **DISCUSSION**

548 Our findings elucidate a strong feedback between plant ecosystem engineers and surface
549 topography at the initial stages of foredune genesis in nebkha formation, both in a wind tunnel
550 and field setting. We show that feedbacks are explained by plant traits. Specifically: (1) larger
551 plants created larger nebkha regardless of species; (2) the anecdotal adage that a taller, steeper
552 plant may build a taller steeper dune, is unsupported at initialization, as stem width in erect
553 grasses better predicted nebkha height than plant height alone; and (3) morphological traits
554 impacted nebkha shape, with the erect grasses *P. amarum* and *A. breviligulata* producing more
555 elongated, planar nebkha than low-lying *C. kobomugi*. These relationships hold true regardless of
556 planting density and configuration, although the staggered configuration produced larger nebkha
557 than non-staggered despite equal formative conditions. For management, these results suggest
558 planting more culms per planting hole and/or larger plants to increase nebkha formation and
559 subsequent sediment volume retention. Using a staggered configuration to the prevailing wind
560 may be most conducive for building larger nebkha more quickly over time while simultaneously
561 initiating rapid formation of a foredune that would buffer upland areas during storm events.

562 *Field Validation*

563 Simulations of natural phenomenon are not always field validated, but should be in a
564 well-constructed experimental design (Dunham and Beaupre, 1998), and our field truthing
565 corroborates our wind tunnel findings. The increased size (area, height, and volume) of field
566 nebkha for *A. breviligulata* and *C. kobomugi* was the main difference from the wind tunnel

567 results, despite the wind tunnel plants having been larger than the field plants. We attribute this
568 difference to field nebkha having increased formation time (>30 minutes), and likely forming
569 over multiple transport events under varied wetting and drying cycles (Czarnes et al., 2000;
570 Maun, 2009; Balke et al., 2014; Zarnetske et al., 2015). Similarly, a recent wind tunnel study
571 achieved nebkha elevations of 2-8 cm, but after allotting several hours of formation, compared to
572 our 30 minute run time (Hesp et al., 2019). Our results suggest that the underlying feedbacks or
573 principals that create variation in nebkha size and shape among species remain true in the field
574 beyond initialization. Longer flow-parallel elongation in the field despite likely stems from
575 differences in wind velocity and stem width, which have been shown to impact shadow dune
576 length (Hesp and Smyth, 2017). While field and wind tunnel plant stem widths were equivalent,
577 the speeds of the formative field winds were unknown. Corroboration of the field and wind
578 tunnel results show our findings are ecologically relevant and replicated in natural ecosystems.

579 *The Effect of Plant Morphology on Nebkha Size and Shape*

580 Larger plants formed larger nebkha both in the field and wind tunnel with nuances in
581 variations. Until now, the theory that larger plants build larger aeolian forms, such as foredunes
582 was based entirely on observations of larger plants concomitantly occurring on larger dunes
583 (Davies, 1980; Hesp, 1989; Wootton et al., 2005; Hilton et al., 2006; Hacker et al., 2011, 2019)
584 with some exceptions (Charbonneau et al., 2017). Results presented here highlight the underlying
585 feedbacks contributing to these associations and mirror findings surrounding artificial nebkha
586 shapes where larger nebkha produced larger shadow dunes in their lee (Hesp and Smyth, 2017).
587 This is similar to larger nebkha being established in the field around larger plant assemblages
588 (Gillies et al., 2014). Compared to the aforementioned studies (Davies, 1980; Hesp, 1989;
589 Wootton et al., 2005; Hilton et al., 2006; Hacker et al., 2011; Gillies et al., 2014; Hesp and

590 Smyth, 2017; Hacker et al., 2019), we have reduced the scale to foredune initiation in nebkha
591 genesis (Walker et al., 2017), and elucidated some of the drivers of the underlying feedbacks that
592 enable larger plants to produce greater deposition.

593 At foredune initiation, the inherent morphological traits of the species influenced nebkha
594 shape. Low-lying *C. kobomugi* produced more equant nebkha than erect grasses, supporting the
595 notion that erect grasses, such as *A. breviligulata* are associated with taller and steeper foredunes
596 (Davies, 1980; Wootton et al., 2005; Hacker et al., 2019). This relationship may carry through the
597 life of the evolving foredune as suggested by comparing the lower platform-like established
598 dunes of *Spinifex sericeus* versus *A. breviligulata* (Davies, 1980). Both are erect grasses, but
599 their inflorescences are very different with that of *S. sericeus* being larger, shorter, and splaying
600 horizontally ultimately driving differences in dune morphology (Davies, 1980). The results are
601 consistent with nebkha length increasing with greater porosity, as observed with mesh objects
602 (Gillies et al., 2017) as well as emergent and submerged vegetation (Yagci et al., 2016). Taller
603 plants produce streamlined airflow and deposition around objects as shown by manipulating low-
604 stem leaves on artificial erect plants (Hesp et al., 2019). In contrast, the low-lying stature of *C.*
605 *kobomugi* has reduced porosity which should create increased turbulent kinetic energy and blade
606 motion below the canopy, pushing topography into non-streamlined states (Raupach et al., 1996;
607 Luhar and Nepf, 2013; Boothroyd et al., 2016). Our wind tunnel results match studies of shrubs
608 having increased deposition width and decrease deposition length with increasing horizontal
609 complexity in low-lying leaves (Leenders et al., 2011).

610 Nebkha height was unrelated to plant height or size. Among the erect grasses, *Panicum*
611 built larger nebkha regardless of which grass was taller, while *Carex* and *Ammophila* nebkha
612 were of equivalent height regardless of *Ammophila* being taller (Fig. 5 and 7). At the foredune

613 level, crest height differences are attributed to vegetation height where lower profile plants have
614 been noted (Davies, 1980; Hesp, 1989; Wootton et al., 2005; Hilton et al., 2006) or quantified on
615 shorter established foredunes (Hacker et al., 2011 and 2019). However, greater plant height also
616 tends to coincide with greater biomass and surface cover, both of which create increased trapping
617 efficiency (de M Luna et al., 2011; Zarnetske et al., 2012) as exhibited here in *P. amarum*, but
618 not *A. breviligulata*. This is interesting given that *P. amarum* and *A. breviligulata* have been
619 found on dunes of similar size and shape in nature (Woodhouse et al., 1977; Hacker et al., 2019),
620 but is also important to note that the species currently on a dune may not have necessarily built it
621 (Charbonneau et al., 2017). Sediment size across locations may confound topographic variability
622 created by plant morphology in nature as it can impact nebkha height, but this can be controlled
623 for in a laboratory setting (Hesp, 1981; Hesp and Smyth, 2017). Greater stem width, which
624 equates to greater basal/frontal area and has varies between species (Mullins et al., 2019),
625 appears to be the paramount reason why *P. amarum* and *A. breviligulata* differed in nebkha
626 height. This suggests that in foredune initiation, species identity may play a greater role than at
627 higher densities due to reduced neighbor interaction and basal/frontal area (Pietri et al., 2009).

628 Sediment volume distribution, windward (sedge) versus leeward (erect grasses) of a plant
629 is attributable to plant morphology and height. This finding supports wider stem bases creating
630 longer wake zones (Hesp, 1989), and overlapping wake zones leeward of erect plants having the
631 potential to cause localized scour (Burri et al., 2011; Leenders et al., 2011). Instances of *C.*
632 *kobomugi* windward scouring are also likely due leaf splay at the sediment surface increasing
633 bed turbulence (Burri et al., 2011; Leenders et al., 2011; Luhar and Nepf, 2013). However, the
634 leaf ends of *C. kobomugi* often became buried, no longer moving in the airstream, thus limiting
635 blade motion that could trigger erosion and inciting deposition both upwind and downwind

636 around the entirety of the relatively sheltered plant base (Pietri et al., 2009). Leaf flexibility, not
637 measured here, relative to height and number of leaves, likely also impacts deposition as in air
638 and water flow fields (Järvelä, 2002; Burri et al., 2011; Luhar and Nepf, 2013). The splayed and
639 low-lying semi-rosette shape of *C. kobomugi* may also enable it to better retain accumulated
640 grains (Charbonneau et al., 2016) than other plants (*A. breviligulata* = *C. kobomugi* nebkha
641 volume). However, in the field, this phenomenon must be viewed in the context of how little
642 sediment depth it takes to bury *C. kobomugi* relative to the taller erect grasses.

643 *The Effect of Planting Configuration and Density on Nebkha Size*

644 A staggered planting configuration produced nebkha with twice the volume of a non-
645 staggered configuration. This is an important finding for coastal management and planting
646 efforts. To our knowledge, managers have noted depositional differences from fencing
647 configurations, but have noted no depositional differences from varying plant configuration;
648 however, wind direction, which undoubtedly contributes to deposition variation was not
649 measured concomitantly (Savage and Woodhouse, 1968; Wootton et al., 2016). A staggered
650 planting pattern relative to the prevailing wind direction eliminates or reduces wind alleys
651 through rows, thereby increasing turbulent wake interactions between individuals and inducing
652 greater deposition (Pietri et al., 2009). Regardless of configuration or density, deposition did not
653 vary with plant row, indicating that sediment transported evenly throughout the stand and did not
654 accumulate more in the first upwind or last downwind row as might have been expected from
655 changes in basal/frontal area (Hesp, 1983 and 1989; Arens et al., 2001; Hesp et al., 2019).

656 Unexpectedly, density did not impact nebkha size. More objects theoretically equate to an
657 increased roughness factor and greater wind dampening due to turbulence inducing deposition
658 (Hesp, 1983 and 1989; Zarnetske et al., 2012; Ortiz et al., 2013; Keijsers et al., 2014) and

659 differing densities between species can sometimes exacerbate topographic species-effects in
660 developed foredunes, even in similarly erect grasses (Hacker et al., 2019). Lower densities often
661 facilitate erosion (Keijsers et al., 2016) although they can, in some instances, enhance deposition
662 (Burri et al., 2011). Our results are consistent with research on submerged and non-submerged
663 vegetation, where flow reduction and deposition did not vary by density (Järvelä, 2002; Burri et
664 al., 2011). Our two common management planting densities may not have been different enough
665 to produce density-specific erosive or accretive effects. There may also be no correlation
666 between vegetation density and accretion quantity, as has been suggested at the scale of an
667 established foredune system and the timescale of years (Keijsers et al., 2015). However, our
668 unanalyzed high density treatments forming melded nebkha among groups of plants suggests
669 otherwise. Planting lower densities of larger plants may translate to equivalent accumulation as
670 planting a greater number of smaller plants, but at reduced effort and monetary cost. Similarly, a
671 30.5 cm spacing, may represent a critical density, as has been suggested by Price (1961), below
672 which roughness elements act independently instead of collectively.

673 *Suggestions For Future Research*

674 More is known about the effect of wind on rigid, submerged, and emergent vegetation
675 than on flexible roughness elements or live plants (Järvelä, 2002; Burri et al., 2011). However,
676 solid versus porous obstructions do not behave equivalently in flow conditions (Gillies et al.,
677 2014). Plants undergo streamlining and compression, yielding more heterogeneous velocity
678 fields than solid objects (Boothroyd et al., 2016; Yagci et al., 2016). *In situ* field experiments
679 examining the ecosystem engineers that induce ecogeomorphic responses may thus yield
680 different results than artificial proxies. The use of organic plant root proxies (Bryant et al., 2019)
681 and live plants has recently been applied to simulate laboratory storm beach and dune wave-

682 runup although in studies using live plants it is critical that the plants be fully rooted and
683 established as they would be naturally otherwise the results may hold little bearing on reality
684 (Silva et al., 2016; Feagin et al., 2019). Future endeavors on live plant material could incorporate
685 irregularity in stand configuration as has been done with rigid pegs (Raupach et al., 2006) and
686 artificial flexible plant proxies (Hesp et al., 2019). Additionally, the inclusion of heterogenous
687 species assemblages and the correlation to turbulence generated at the canopy top versus stem-
688 level would bolster the applicability of laboratory studies to natural settings (Nepf et al., 2007).

689 Ecogeomorphic sandy dune ecosystems across coastlines share many of the same
690 anthropogenic challenges and functional similarity such that this research can contribute to a
691 global framework for management and restoration of coastal interface habitats as suggested by
692 Balke et al. (2014) and Corenblit et al. (2015). Scale constraints exist when studying beach-dune
693 system evolution (Walker et al., 2017) and beach-dune research is often geologically focused
694 (Jackson and Nordstrom, 2019). However, a more interdisciplinary approach, as applied here,
695 appears needed to encapsulate the variability surrounding inherently complex ecogeomorphic
696 systems (Stallins, 2006; Walker et al. 2017; Stallins and Corenblit, 2018). Ecogeomorphic
697 systems are interdisciplinary by their very nature and as such, future research should seek to span
698 disciplines and field-validated laboratory experiments when broaching topics with management
699 implications (Stallins, 2006, Schlacher et al., 2008; Murray et al., 2008; Corenblit et al., 2011;
700 Stallins and Corenblit, 2018). Integrative ecogeomorphic studies have the potential to yield more
701 realistic results of complex natural associations and thus more concrete suggestions for
702 management by virtue of their improved systems perspective.

703 **CONCLUSIONS**

704 This research contributes to our fundamental understanding of the role of intraspecific
705 variation in vegetation morphology, density, and configuration to impact geomorphological
706 processes in aeolian beach-dune systems. We demonstrated that larger plants built larger nebkha,
707 lending experimental support to the commonly held belief that larger plants build larger
708 foredunes. However, taller plants do not necessarily build taller and steeper nebkha. Rather, stem
709 width, a proxy for basal/frontal area, appears to better predict nebkha height. Differences in
710 volumetric accumulation are directly dependent upon stand configuration relative to the
711 prevailing wind direction. Planiform nebkha shape is unrelated to biomass and instead varied
712 with species morphology with low-lying *C. kobomugi* producing more equant nebkha than both
713 erect grasses. We focused on small-scale fundamental processes with applications to improve
714 system scale predictions and modeling in future work. The field validation effort supported the
715 laboratory-observed ecogeomorphic foredune initiation feedbacks, and suggested that these
716 relationships are maintained as the nebkha grows. The results have inherent management and
717 modeling applications for species-specific vegetation parameterization to improve our
718 understanding of spatiotemporal foredune evolution and recovery, storm response, and system
719 state. These results suggest that planting more culms per hole and larger plants staggered to the
720 prevailing wind direction will result in more rapid accumulation which can translate to reduced
721 dune formation time. For modeling, we provide evidence of plants acting as ecosystem engineers
722 in foredune habitats such that they should not be excluded as factors in modeling efforts. These
723 results can be used for vegetation parameterization to yield more robust model results and
724 provide a basis for testing hypotheses generated at the larger foredune scale. Understanding the
725 efficacy of natural dune engineers will only be increasingly important as climate change and sea
726 level rise impose heightened stress on critical ecogeomorphic habitats worldwide.

727

728 **AUTHOR CONTRIBUTIONS**

729 Charbonneau secured funding to build the wind tunnel and conduct the research working, with
 730 Zarnetske designing its specifications based on previous blueprints. Wnek secured the wind
 731 tunnel location, and worked with students and Charbonneau collecting data. Charbonneau
 732 organized and oversaw the wind tunnel construction and carried out the research. Zarnetske,
 733 Wnek, Casper, and Barber each contributed to experimental design. Dohner and Charbonneau
 734 conducted field validation analyses. All authors contributed to the final manuscript.

735

736

737

738 **ACKNOWLEDGEMENTS**

739 This research was conducted with Government support under contract FA9550-11-C-0028 and
 740 awarded by the Department of Defense, Air Force Office of Scientific Research, National
 741 Defense Science and Engineering Graduate (NDSEG) Fellowship, 32 CFR 168a. The wind
 742 tunnel was funded and supported by the US Coastal Research Program (USCRP) with USACE
 743 ERDC and USGS (Contract #W912HZ18P0090) organized by the American Shore and Beach
 744 Preservation Society and USACE ERDC BAA CHL-15 (Contract #W912HZ-16-P-0088). The
 745 following entities within New Jersey donated resources without which the wind tunnel would not
 746 exist: NJDEP, Island Beach State Park, NJ FWS, NJ Ocean County School (OCVTS) Board, and
 747 Marine Academy of Technology and Environmental Studies (MATES). We Ed Crawford and
 748 Anthony Reo, as well as the following local and national sponsors that donated invaluable
 749 resources and expertise: Air Systems Engineering, Coastal Transplants, HandyMan Pros, Motion
 750 Industries, Moxley Electronics, One Ton Bag LLC, Pineland's Nursery, EMCO Industrial
 751 Plastics, and SICK Sensor Intelligence. Peter Petraitis and Arthur Dunham are thanked for
 752 statistical expertise.

753

754

755 **LITERATURE CITED**

756

757 AgiSoft. 2018. Agisoft Metashape User Manual - Professional Edition, Version 1.5. Pages 1–
 758 130.

759 Arens, S.M. 1996. Patterns of sand transport on vegetated foredunes. *Geomorphology* 17:339–
 760 350.

761 Arens, S.M., A. Baas, J.H. Van Boxel, and C. Kalkman. 2001. Influence of reed stem density on
 762 foredune development. *Earth Surface Processes and Landforms* 26:1161–1176.

763 Badano, E.I., and L.A. Cavieres. 2006. Impacts of ecosystem engineers on community attributes:
 764 effects of cushion plants at different elevations of the Chilean Andes. *Diversity Distributions*
 765 12:388–396.

766 Balke, T., P.M.J. Herman, and T.J. Bouma. 2014. Critical transitions in disturbance-driven
 767 ecosystems: identifying Windows of Opportunity for recovery. *Journal of Ecology* 102:700–
 768 708.

769 Bauer, B.O., C.A. Houser, and W.G. Nickling. 2004. Analysis of velocity profile measurements
 770 from wind-tunnel experiments with saltation. *Geomorphology* 59:81–98.

- 771 Bendix, J., and C.R. Hupp. 2000. Hydrological and geomorphological impacts on riparian plant
772 communities. *Hydrological Processes* 14:2977–2990.
- 773 Boothroyd, R.J., R.J. Hardy, J. Warburton, and T.I. Marjoribanks. 2016. The importance of
774 accurately representing submerged vegetation morphology in the numerical prediction of
775 complex river flow. *Earth Surface Processes and Landforms* 41:567–576.
- 776 Bos, A.R., T.J. Bouma, G.L.J. de Kort, and M.M. van Katwijk. 2007. Ecosystem engineering by
777 annual intertidal seagrass beds: Sediment accretion and modification. *Estuarine, Coastal and*
778 *Shelf Science* 74:344–348.
- 779 Bryant, D.B., Bryant, M.A., Sharp, J.A., Bell, G.L., and Moore C. 2019. The response of
780 vegetated dunes to wave attack. *Coastal Engineering* 152: 103506.
- 781 Burri, K., C. Gromke, M. Lehning, and F. Graf. 2011. Aeolian sediment transport over
782 vegetation canopies: A wind tunnel study with live plants. *Aeolian Research* 3:1–9.
- 783 Charbonneau, B.R., and B.B. Casper. 2018. Wind tunnel tests inform *Ammophila* planting
784 spacing for dune management. *Shore & Beach* 86:37–46.
- 785 Charbonneau, B.R., J.P. Wnek, J.A. Langley, G. Lee, and R.A. Balsamo. 2016. Above vs.
786 belowground plant biomass along a barrier island: Implications for dune stabilization.
787 *Journal of Environmental Management* 182:126–133.
- 788 Charbonneau, B.R., L.S. Wootton, J.P. Wnek, J.A. Langley, and M.A. Posner. 2017. A species
789 effect on storm erosion: Invasive sedge stabilized dunes more than native grass during
790 Hurricane Sandy. *Journal of Applied Ecology* 54:1385–1394.
- 791 Cheplick, G.P. 2016. Changes in plant abundance on a coastal beach following two major storm
792 surges 1. *Journal of the Torrey Botanical Society* 143:180–191.
- 793 Cooke, R.A., Warren, and A. Goudie. 1992. *Desert Geomorphology*. UCL Press, London.
- 794 Carter, R.W.G. 1995. *Coastal environments: an introduction to the physical, ecological and*
795 *cultural systems of coastlines*. 5th ed. Academic Press, London
- 796 Corenblit, D., A. Baas, T. Balke, T. Bouma, F. Fromard, V. Garófano-Gómez, E. González, A.
797 M. Gurnell, B. Hortobágyi, F. Julien, D. Kim, L. Lambs, J. A. Stallins, J. Steiger, E.
798 Tabacchi, and R. Walker. 2015. Engineer pioneer plants respond to and affect geomorphic
799 constraints similarly along water-terrestrial interfaces world-wide. *Global Ecology and*
800 *Biogeography* 24:1363–1376.
- 801 Corenblit, D., A. Baas, G. Bornette, J. Darrozes, S. Delmotte, R.A. Francis, A.M. Gurnell, F.
802 Julien, R.J. Naiman, and J. Steiger. 2011. Feedbacks between geomorphology and biota
803 controlling Earth surface processes and landforms: A review of foundation concepts and
804 current understandings. *Earth-Science Reviews* 106:307–331.
- 805 Cowles, H.C. 1899. The Ecological Relations of the Vegetation on the Sand Dunes of Lake
806 Michigan. *Botanical Gazette* 27:167–202.
- 807 Czarnes, S., P.D. Hallett, A.G. Bengough, and I.M. Young. 2000. Root- and microbial- derived
808 mucilages affect soil structure and water transport. *European Journal of Soil Science*
809 51:435–443.
- 810 Davies, J.L. 1980. *Geographical Variation in Coastal Development*. Longman, London.
- 811 de Castro, F. 1995. Computer simulation of the dynamics of a dune system. *Ecological*
812 *Modelling* 78:205–217.
- 813 de M Luna, M.C.M., E.J.R. Parteli, O. Durán, and H.J. Herrmann. 2011. Model for the genesis of
814 coastal dune fields with vegetation. *Geomorphology* 129:215–224.

- 815 Dohner, S.M., A.C. Trembanis, and D.C. Miller. 2016. A tale of three storms: Morphologic
816 response of Broadkill Beach, Delaware, following Superstorm Sandy, Hurricane Joaquin,
817 and Winter Storm Jonas. *Shore & Beach* 84:1–7.
- 818 Dunham, A.E., and S.J. Beaupre. 1998. Ecological experiments: scale, phenomenology,
819 mechanism, and the illusion of generality. In: Resitarits, W. and Bernardo, J.(eds),
820 *Experimental ecology* Pages 27–49.
- 821 Duran, O., and L.J. Moore. 2013. Vegetation controls on the maximum size of coastal dunes.
822 *Proceedings of the National Academy of Sciences* 110:17217–17222.
- 823 Durán Vinent, O., and L.J. Moore. 2014. Barrier island bistability induced by
824 biophysical interactions. *Nature Climate Change* 5:158–162.
- 825 Elko, N., K. Brodie, H. Stockdon, and K. Nordstrom. 2016. Dune management challenges on
826 developed coasts. *Shore & Beach* 84: 15–28.
- 827 Elko, N., C. Dietrich, M. Cialone, H. Stockdon, M.W. Bilskie, B. Boyd, B.R. Charbonneau, D.
828 Cox, K. Dresback, S. Elgar, et al. 2019. Advancing the understanding of storm processes and
829 impacts. *Shore & Beach* 87: 37–51.
- 830 Emery, S.M., L. Bell-Dereske, and J.A. Rudgers. 2015. Fungal symbiosis and precipitation alter
831 traits and dune building by the ecosystem engineer, *Ammophila breviligulata*. *Ecology*
832 96:927–935.
- 833 Feagin, R.A., M. Furman, K. Salgado, M.L. Martinez, R.A. Innocenti, K. Eubanks, J. Figlus, T.
834 P. Huff, J. Sigren, and R. Silva. 2019. The role of beach and sand dune vegetation in
835 mediating wave run up erosion. *Estuarine, Coastal and Shelf Science* 219:97–106.
- 836 Feagin, R.A., J. Figlus, J.C. Zinnert, J. Sigren, M.L. Martínez, R. Silva, W.K. Smith, D. Cox,
837 D.R. Young, and G. Carter. 2015. Going with the flow or against the grain? The promise of
838 vegetation for protecting beaches, dunes, and barrier islands from erosion. *Frontiers in*
839 *Ecology and the Environment* 13: 203–210.
- 840 Fei, S., J. Phillips, and M. Shouse. 2014. Biogeomorphic impacts of invasive species. *Annual*
841 *Review of Ecology, Evolution, and Systematics* 45:69–87.
- 842 Gares, P.A. 1992. Topographic changes associated with coastal dune blowouts at island beach
843 state park, New Jersey. *Earth Surface Processes and Landforms* 17:589–604.
- 844 Gillies, J.A., J.M. Nield, and W.G. Nickling. 2014. Wind speed and sediment transport recovery
845 in the lee of a vegetated and denuded nebkha within a nebkha dune field. *Aeolian Research*
846 12:135–141.
- 847 Gillies, J.A., W.G. Nickling, G. Nikolich, and V. Etyemezian. 2017. A wind tunnel study of the
848 aerodynamic and sand trapping properties of porous mesh 3-dimensional roughness
849 elements. *Aeolian Research* 25:23–35.
- 850 Goldstein, E.B., L.J. Moore, and O. Durán Vinent. 2017. Vegetation controls on maximum
851 coastal foredune ‘hummockiness’ and annealing time. *Earth Surface Dynamics*
852 *Discussions*:1–15.
- 853 Goldstein, E.B., and L. J. Moore 2016. Stability and bistability in a one-dimensional model of
854 coastal foredune height. *Journal of Geophysical Research: Earth Surface* 121:964–977.
- 855 Graham, M.H. 2003. Confronting multicollinearity in ecological multiple regression. *Ecology*
856 84:2809–2815.
- 857 Hacker, S.D., K.R. Jay, N. Cohn, E.B. Goldstein, P.A. Hovenga, M. Itzkin, L.J. Moore, R.S.
858 Mostow, E.V. Mullins, and P. Ruggiero. 2019. Species-Specific Functional Morphology of
859 Four US Atlantic Coast Dune Grasses: Biogeographic Implications for Dune Shape and
860 Coastal Protection. *Diversity* 11:82–16.

- 861 Hacker, S.D., P. Zarnetske, E. Seabloom, P. Ruggiero, J. Mull, S. Gerrity, and C. Jones. 2011.
 862 Subtle differences in two non-native congeneric beach grasses significantly affect their
 863 colonization, spread, and impact. *Oikos* 121:138–148.
- 864 Hall Cushman, J., J.C. Waller, and D.R. Hoak. 2010. Shrubs as ecosystem engineers in a coastal
 865 dune: influences on plant populations, communities and ecosystems. *Journal of Vegetation*
 866 *Science* 21:821–831.
- 867 Hesp, P.A. 1981. The formation of shadow dunes. *Journal of Sedimentary Petrology* 51:101–
 868 112.
- 869 Hesp, P.A. 1983. Morphodynamics of Incipient Foredues in New South Wales, Australia. Pages
 870 325–342 *in* *Eolian Sediments and Processes*. Elsevier.
- 871 Hesp, P.A. 1984. Foredune formation in SE Australia. In: B.G. Thom (*Ed.*) *Coastal*
 872 *Geomorphology in Australia*, Sydney: Academic Press: 60–97.
- 873 Hesp, P.A. 1989. A review of biological and geomorphological processes involved in the
 874 initiation and development of incipient foredues. *International Association for Scientific*
 875 *Hydrology* 54:181–201.
- 876 Hesp, P.A. 2002. Foredues and blowouts: initiation, geomorphology and dynamics.
 877 *Geomorphology* 48:245–268.
- 878 Hesp, P.A. 2013. A 34 year record of foredune evolution, Dark Point, NSW, Australia. *Journal*
 879 *of Coastal Research* 165:1295–1300.
- 880 Hesp, P.A., Y. Dong, H. Cheng, and J. L. Booth. 2019. Wind flow and sedimentation in artificial
 881 vegetation: Field and wind tunnel experiments. *Geomorphology* 337:165–182.
- 882 Hesp, P.A., M. Martinez, G.M. da Silva, N. Rodríguez-Revelo, E. Gutierrez, A. Humanes, D.
 883 Laínez, I. Montañó, V. Palacios, A. Quesada, L. Storero, G.G. Trilla, and C. Trochine. 2011.
 884 Transgressive dunefield landforms and vegetation associations, Doña Juana, Veracruz,
 885 Mexico. *Earth Surface Processes and Landforms* 36:285–295.
- 886 Hesp, P.A., and T.A.G. Smyth. 2017. Nebkha flow dynamics and shadow dune formation.
 887 *Geomorphology* 282:27–38.
- 888 Hesp, P.A., T.A.G. Smyth, P. Nielsen, I.J. Walker, B.O. Bauer, and R. Davidson-Arnott. 2015.
 889 Flow deflection over a foredune. *Geomorphology* 230:64–74.
- 890 Hesp, P.A., and I. J. Walker. 2013. Coastal dunes. In: Shroder, J. (Editor in Chief), Lancaster, N.,
 891 Sherman, D.J., Baas, A.C.W. (Eds.), *Treatise on Geomorphology*. Academic Press, San
 892 Diego, CA, vol. 11, *Aeolian Geomorphology*, pp. 328–355.
- 893 Hilton, M., N. Harvey, A. Hart, K. James, and C. Arbuckle. 2006. The impact of exotic dune
 894 grass species on foredune development in Australia and New Zealand: a case study of
 895 *Ammophila arenaria* and *Thinopyrum junceiforme*. *Australian Geographer* 37:313–334.
- 896 Houser, C. 2013. Alongshore variation in the morphology of coastal dunes: Implications for
 897 storm response. *Geomorphology* 199:48–61.
- 898 Houser, C., C. Hapke, and S. Hamilton. 2008. Controls on coastal dune morphology, shoreline
 899 erosion and barrier island response to extreme storms. *Geomorphology* 100:223–240.
- 900 Houser, C., and S. Mathew. 2011. Alongshore variation in foredune height in response to
 901 transport potential and sediment supply: South Padre Island, Texas. *Geomorphology* 125:62–
 902 72.
- 903 Intelligence, S. S. 2019. *TriSpector1000 Operating Instructions*:1–104.
- 904 Jackson, N.L., and K.F. Nordstrom. 2019. Trends in research on beaches and dunes on sandy
 905 shores, 1969-2019. *Geomorphology*:1–13.
- 906 Järvelä, J. 2002. Flow resistance of flexible and stiff vegetation: a flume study with natural

- 907 plants. *Journal of Hydrology* 269:44–54.
- 908 JMP®. 2019. Version Pro 14. SAS Institute Inc., Cary, NC.
- 909 Johnson, E.A., and K. Miyanishi. 2007. Disturbance and Succession. Pages 1–14 *in* Plant
910 Disturbance Ecology.
- 911 Jones, C.G. 2012. Ecosystem engineers and geomorphological signatures in landscapes.
912 *Geomorphology* 157-158:75–87.
- 913 Jones, C.G., J.H. Lawton, and M. Shachak. 1994. Organisms as Ecosystem Engineers. *Oikos*
914 69:373–386.
- 915 Jones, C.G., J.H. Lawton, and M. Shachak. 1997. Positive and negative effects of organisms as
916 physical ecosystem engineers. *Ecology* 78:1946–14.
- 917 Keijsers, J.G.S., A.V. De Groot, and M.J.P.M. Riksen. 2015. Vegetation and sedimentation on
918 coastal foredunes. *Geomorphology* 228:723–734.
- 919 Keijsers, J.G.S., A.V. De Groot, and M.J.P.M. Riksen. 2016. Modeling the biogeomorphic
920 evolution of coastal dunes in response to climate change. *Journal of Geophysical Research*
921 *Earth Surface* 121:1161–1181.
- 922 Keijsers, J.G.S., A. Poortinga, M.J.P.M. Riksen, and J. Maroulis. 2014. Spatio-temporal
923 variability in accretion and erosion of coastal foredunes in the Netherlands: regional climate
924 and local topography. *PLoS ONE* 9:e91115.
- 925 Leenders, J.K., G. Sterk, and J.H. Van Boxel. 2011. Modelling wind-blown sediment transport
926 around single vegetation elements. *Earth Surface Processes and Landforms* 36:1218–1229.
- 927 Luhar, M., and H.M. Nepf. 2013. From the blade scale to the reach scale: A characterization of
928 aquatic vegetative drag. *Advances in Water Resources* 51:305–316.
- 929 MathWorks, Inc. 2018. MATLAB and Statistics and Machine Learning Toolbox Release 2018a,
930 The MathWorks, Inc., Natick, Massachusetts, United States.
- 931 Maun, M.A. 2009. *The biology of coastal sand dunes*. Oxford, UK: Oxford University Press.
- 932 Min, B.M. 2006. Shoot growth and distribution pattern of *Carex kobomugi* in a natural stand.
933 *Journal of Plant Biology* 49:224–230.
- 934 Moore, L.J., O. Durán Vinent, and P. Ruggiero. 2016. Vegetation control allows autocyclic
935 formation of multiple dunes on prograding coasts. *Geology*:G37778.1–4.
- 936 Mullins, E., L. J. Moore, E.B. Goldstein, T. Jass, J. Bruno, and O. Durán Vinent. 2019.
937 Investigating dune- building feedback at the plant level: Insights from a multispecies field
938 experiment. *Earth Surface Processes and Landforms* 60: 205–14.
- 939 Murray, A.B., M.A.F. Knaapen, M. Tal, and M.L. Kirwan. 2008. Biomorphodynamics: Physical-
940 biological feedbacks that shape landscapes. *Water Resources Research* 44:W11301.
- 941 Nield, J.M., and A.C. Baas. 2008. Investigating parabolic and nebkha dune formation using a
942 cellular automaton modelling approach. *Earth Surface Processes and Landforms* 33: 724–
943 740.
- 944 Nepf, H., M. Ghisalberti, B. White, and E. Murphy. 2007. Retention time and dispersion
945 associated with submerged aquatic canopies. *Water Resources Research* 43:n/a–n/a.
- 946 O'Connell, J. 2008. Coastal dune protection and restoration, using “Cape” American beachgrass
947 and fencing. Pages 1–17. Woods Hole Sea Grant and Barnstable County Cooperative
948 Extension Service.
- 949 Ortiz, A.C., A. Ashton, and H. Nepf. 2013. Mean and turbulent velocity fields near rigid and
950 flexible plants and the implications for deposition. *Journal of Geophysical Research: Earth*
951 *Surface* 118:2585–2599.

- 952 Pietri, L., A. Petroff, M. Amielh, and F. Anselmet. 2009. Turbulence characteristics within
953 sparse and dense canopies. *Environmental Fluid Mechanics* 9:297–320.
- 954 Price, W.I.J. 1961. The effects of the characteristics of snow fences on the quantity and shape of
955 the deposited snow. *Agriculture, Ecosystems & Environment* 22-23:89–98.
- 956 Ranwell, D.S. 1972. *Ecology of salt marshes and sand dunes*. Chapman and Hall, London.
- 957 Raupach, M.R. 1992. Drag and drag partition on rough surfaces. *Boundary-Layer Meteorology*
958 60:375–395.
- 959 Raupach, M.R., J.J. Finnigan, and Y. Brunei. 1996. Coherent eddies and turbulence in vegetation
960 canopies: The mixing-layer analogy. *Boundary-Layer Meteorology* 78:351–382.
- 961 Raupach, M.R., D.E. Hughes, and H.A. Cleugh. 2006. Momentum Absorption in Rough-Wall
962 Boundary Layers with Sparse Roughness Elements in Random and Clustered Distributions.
963 *Boundary-Layer Meteorology* 120:201–218.
- 964 Savage, R.P., and W.W. Woodhouse. 1968. Creation and stabilization of coastal barrier dunes.
965 *Coastal Engineering*.
- 966 Schlacher, T.A., D.S. Schoeman, J. Dugan, M. Lastra, A. Jones, F. Scapini, and A. McLachlan.
967 2008. Sandy beach ecosystems: key features, sampling issues, management challenges and
968 climate change impacts. *Marine Ecology* 29:70–90.
- 969 Seneca, E.D., W.W. Woodhouse, and S.W. Broome. 1976. Dune stabilization with *Panicum*
970 *amarum* along the North Carolina coast.
- 971 Silva, R., M.L. Martínez, I. Odériz, E. Mendoza, and R. A. Feagin. 2016. Response of vegetated
972 dune-beach systems to storm conditions. *Coastal Engineering* 109:53–62.
- 973 Stallins, J.A. 2005. Stability domains in barrier island dune systems. *Ecological Complexity*
974 2:410–430.
- 975 Stallins, J.A. 2006. Geomorphology and ecology: Unifying themes for complex systems in
976 biogeomorphology. *Geomorphology* 77:207–216.
- 977 Stallins, J.A., and D. Corenblit. 2018. Interdependence of geomorphic and ecologic resilience
978 properties in a geographic context. *Geomorphology* 305:76–93.
- 979 Tanaka, N., N.A.K. Nandasena, K.B.S.N. Jinadasa, Y. Sasaki, K. Tanimoto, and M.I.M.
980 Mowjood. 2009. Developing effective vegetation bioshield for tsunami protection. *Civil*
981 *Engineering and Environmental Systems* 26:163–180.
- 982 Tanner, C.C. 2001. Plants as ecosystem engineers in subsurface-flow treatment wetlands. *Water*
983 *science and technology : a journal of the International Association on Water Pollution*
984 *Research* 44:9–17.
- 985 Van Dijk, P.M., S.M. Arens, and J.H. Van Boxel. 1999. Aeolian processes across transverse
986 dunes. II: Modelling the sediment transport and profile development. *Earth Surface*
987 *Processes and Landforms* 24: 319–333.
- 988 Walker, I.J., R.G.D. Davidson-Arnott, B.O. Bauer, P.A. Hesp, I. Delgado-Fernandez, J.
989 Ollerhead, and T.A.G. Smyth. 2017. Scale-dependent perspectives on the geomorphology
990 and evolution of beach-dune systems. *Earth-Science Reviews* 171:220–253.
- 991 Wolner, C.W.V., Moore, L.J., Young, D.R., Brantley, S.T., Bissett, S.N., McBride, R.A. 2013.
992 Ecomorphodynamic feedbacks and barrier island response to disturbance: Insights from the
993 Virginia Barrier Islands, Mid-Atlantic Bight, USA. *Geomorphology* 199: 115–128.
- 994 Woodhouse, W.W., E.D. Seneca Jr, and S.W. Broome. 1977. Effect of species on dune grass
995 growth 21:256–266.
- 996 Woodhouse, W.W., Jr. 1982. Coastal sand dunes of the US. Pages 1–43 in R. R. Lewis, editor.
997 *Creation and Restoration of Coastal Plant Communities*. CRC Press, Boca Raton, FL.

- 998 Wootton, L.S., S.D. Halsey, K. Bevaart, A. McGough, J. Ondreicka, and P. Patel. 2005. When
999 invasive species have benefits as well as costs: managing *Carex kobomugi* (Asiatic sand
1000 sedge) in New Jersey's coastal dunes. *Biological Invasions* 7:1017–1027.
- 1001 Wootton, L., J. Miller, C. Miller, M. Peek, A. Williams, and P. Rowe. 2016. NJ Sea Grant
1002 Consortium Dune Manual. Pages 1–77.
- 1003 Yagci, O., M.F. Celik, V. Kitsikoudis, V.S.O. Kirca, C. Hodoglu, M. Valyrakis, Z. Duran, and S.
1004 Kaya. 2016. Scour patterns around isolated vegetation elements. *Advances in Water*
1005 *Resources* 97:251–265.
- 1006 Zarnetske, P.L., P. Ruggiero, E.W. Seabloom, and S.D. Hacker. 2015. Coastal foredune
1007 evolution: the relative influence of vegetation and sand supply in the US Pacific Northwest.
1008 *Journal of The Royal Society Interface* 12:20150017–20150017.
- 1009 Zarnetske, P.L., S.D. Hacker, E.W. Seabloom, P. Ruggiero, J.R. Killian, T.B. Maddux, and D.
1010 Cox. 2012. Biophysical feedback mediates effects of invasive grasses on coastal dune shape.
1011 *Ecology* 93:1439–1450.
- 1012 Zhang, W., R. Schneider, J. Kolb, T. Teichmann, J. Dudzinska-Nowak, J. Harff, and T.J.J.
1013 Hanebuth. 2015. Land–sea interaction and morphogenesis of coastal foredunes — A
1014 modeling case study from the southern Baltic Sea coast. *Coastal Engineering* 99:148–166.
1015
1016